Article

Designing Anti-inflammatory Drugs from Parasitic Worms: A Synthetic Small Molecule Analogue of the *Acanthocheilonema viteae* Product ES-62 Prevents Development of Collagen-Induced Arthritis

Lamyaa Al-Riyami,[†,ǁ] Miguel A. Pineda,[‡,ǁ] Justyna Rzepecka,[†,ǁ] Judith K. Huggan,[§] Abedawn I. Khalaf,[§] Colin J. Suckling,[§] Fraser J. Scott,[§] David T. Rodgers,[‡] Margaret M. Harnett,[‡] and William Harnett*[,†]

[†]Strathclyde Institute of Pharmacy and Biomedical Sciences, University of Strathclyde, 161 Cathedral Street, Glasgow G4 0RE, U.K.
[‡]Institute of Infection, Immunity and Inflammation, University of Glasgow, Glasgow G12 8TA, U.K.
[§]Department of Pure and Applied Chemistry, University of Strathclyde, Glasgow G1 1XL, U.K.

Ⓢ Supporting Information

ABSTRACT: In spite of increasing evidence that parasitic worms may protect humans from developing allergic and autoimmune diseases and the continuing identification of defined helminth-derived immunomodulatory molecules, to date no new anti-inflammatory drugs have been developed from these organisms. We have approached this matter in a novel manner by synthesizing a library of drug-like small molecules based upon phosphorylcholine, the active moiety of the anti-inflammatory *Acanthocheilonema viteae* product, ES-62, which as an immunogenic protein is unsuitable for use as a drug. Following preliminary in vitro screening for inhibitory effects on relevant macrophage cytokine responses, a sulfone-containing phosphorylcholine analogue (**11a**) was selected for testing in an in vivo model of inflammation, collagen-induced arthritis (CIA). Testing revealed that **11a** was as effective as ES-62 in protecting DBA/1 mice from developing CIA and mirrored its mechanism of action in downregulating the TLR/IL-1R transducer, MyD88. **11a** is thus a novel prototype for anti-inflammatory drug development.

ES-62
Immunomodulatory
Protein with PC

Anti-inflammatory
small molecule.
Prototype drug.
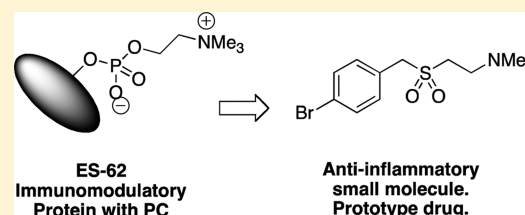
INTRODUCTION

Parasitic helminths infect up to one-third of the global population[1] due to having evolved numerous strategies to balance their survival with that of the host. One mechanism employs secretion of molecules that subtly modulate the host immune response (review ref 2) to prevent clearance of the parasite without leaving the host vulnerable to opportunistic infections. An understanding of the molecular aspects of this mechanism has been approached through characterization of molecules such as ES-62, a protein discovered in the secretions of the rodent filarial nematode *Acanthocheilonema viteae*.[3] ES-62 has a range of immunomodulatory effects, many of which involve subversion of TLR4 signaling to induce an anti-inflammatory immunological phenotype.[4−6] The molecule has therefore been studied for its therapeutic potential in human diseases associated with aberrant inflammation such as rheumatoid arthritis (RA) and has been found to be protective in the mouse model of RA, collagen-induced arthritis (CIA), via targeting of pathogenic pro-inflammatory cytokines, in particular IL-17 and IFNγ.[7−9]

As a tetrameric protein of ∼240 kDa (review ref 10), ES-62 is immunogenic and hence unsuitable for use as a drug. However, key anti-inflammatory activities are associated with its post-translational glycosylation and subsequent esterification by phosphorylcholine (PC; review ref 11). Thus, the development of low molecular weight, nonimmunogenic, PC-based deriva-tives demonstrating ES-62-like biological properties might offer

a better approach to drug discovery. Indeed, we have previously found that short synthetic peptides containing PC-esters of tyrosine as well as PC-containing glycosphingolipids replicate some of the immunomodulatory properties of ES-62 in vitro[12−15] (and unpublished results). Here, we describe the design and synthesis of a library of novel small molecule analogues (SMAs) related to PC and provide proof of concept in the in vivo CIA model that such compounds can be active against inflammatory diseases like RA for which improved drugs are sought.

Initially, the SMAs were screened in vitro to determine their effect on pro-inflammatory cytokines, promoting Th1 (IFNγ)/Th17 (IL-17) responses that are secreted by macrophages in response to pathogen-associated molecular patterns (PAMPs). The screening strategy was chosen, not only because of the pathogenic roles ascribed to Th1/Th17 polarizing cytokines in RA but also because TLRs are highly expressed by fibroblasts and macrophages in the synovium, and synovial expression of TLR2, TLR4, and TLR9 is further upregulated by IL-17 (in an IL-1β and IL-6-dependent manner) in CIA.[16] Indeed, recent studies suggest that elevated TLR2 levels contribute to the spontaneous release of pro-inflammatory cytokines by synovial tissues.[17] Moreover, production of pro-inflammatory chemo-kines, cytokines, and matrix metalloproteinases, as well as
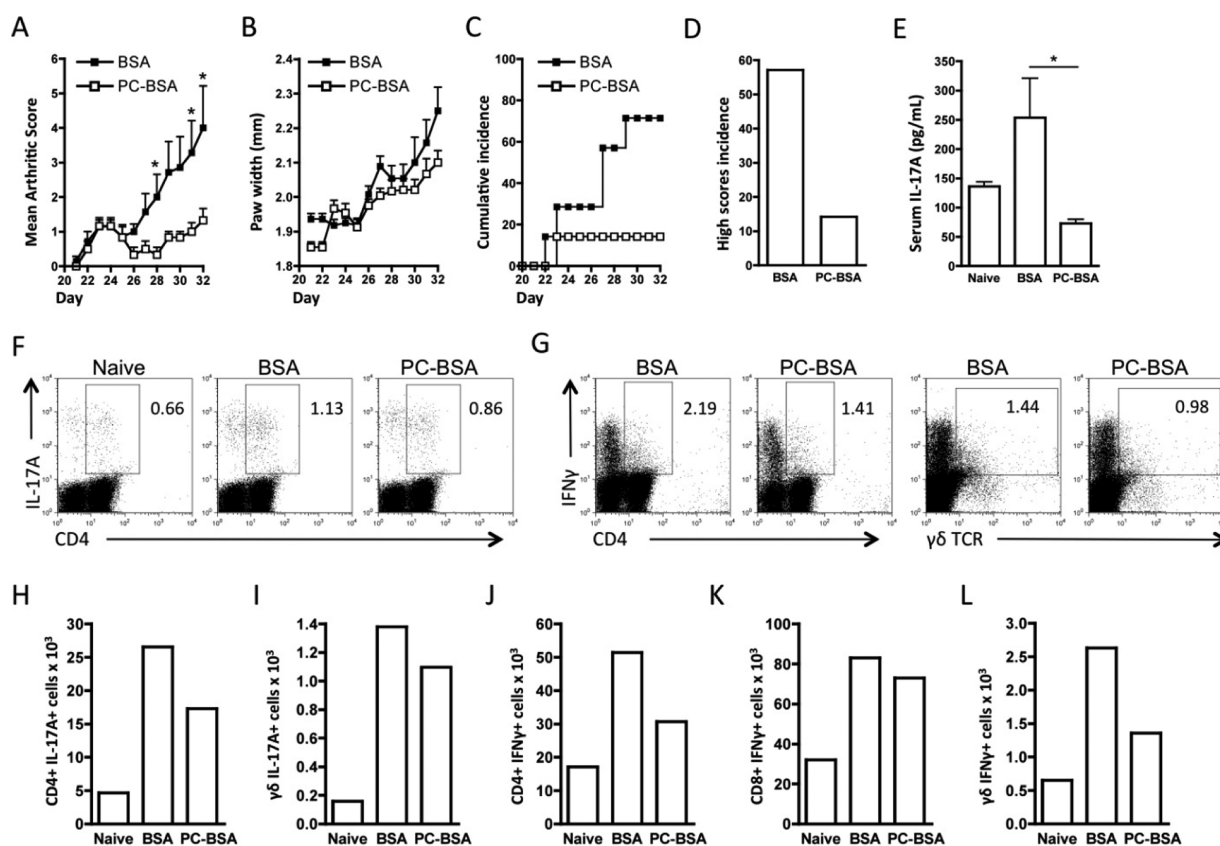
Figure 1. PC-BSA protects against CIA and targets IL-17 and IFNγ responses. Arthritis scores (BSA, $n = 7$; PC-BSA, $n = 6$ (A)) and hind paw width (B), expressed as mean scores ± SEM for BSA- or PC-BSA-treatment groups where n = number of individual mice exposed to collagen and disease incidence (C,D), indicated by the % of mice developing a severity score ≥2 (C) or ≥4 (D). Serum IL-17 levels are plotted as mean values of triplicate IL-17 analyses of serum from individual mice (naïve, $n = 3$; BSA, $n = 6$; PC-BSA, $n = 6$ (E)). (F,G) Exemplar plots of gating strategy of intracellular IL-17 and IFNγ expression by DLN (draining lymph node) cells pooled from BSA- and PC-BSA-treated mice with CIA show CD4 or γδ expression on the x-axis versus cytokine expression on the y-axis, with the relevant % cytokine positive cells annotated. The numbers of cytokine-expressing $CD4^+$ T cells (H,J), γδ T cells (I,L), and $CD8^+$ T cells (K) present in the pooled DLN cells from the naïve (not exposed to collagen), BSA, and PC-BSA groups are shown. For statistical analysis, *$p < 0.05$.

promotion of angiogenesis and cellular invasion[18] and also decreases in matrix biosynthesis,[19] can be stimulated by triggering of TLRs by PAMPs or endogeneous damage-associated molecular patterns (DAMPs) that are present in synovial tissue of patients (e.g., TLR2, gp96, Snapin; TLR4, HSP22, tenascin-C). It has thus been proposed that such aberrant TLR signaling drives the chronic inflammation characteristic of RA (reviews refs 20−22). Collectively, these data have contributed to the identification of TLRs as therapeutic targets in inflammatory disease.[23] Hence our previous findings that ES-62 exerts its anti-inflammatory effects at least in part by subverting TLR4 signaling to suppress TLR2, TLR4, and TLR9 responses suggests this screening approach for novel RA-targeted drugs is appropriate.[4,5] Thus, following the in vitro screen, we selected one of the molecules with properties most similar to ES-62, a sulfone (**11a**) (termed S3 in UK Patent Application No. 1214106.5) for testing in the CIA model.

■ RESULTS

PC Conjugated to Bovine Serum Albumin (PC-BSA) Mimics ES-62 in Suppressing IL-17 and IFNγ Responses in CIA. RA has been proposed to exhibit a Th1/Th17 phenotype of autoimmune inflammation, and we have recently shown that ES-62 suppresses both IFNγ and IL-17 production

in CIA. While we previously showed that the parasite product modulates Th1 responses by suppression of their priming by dendritic cells (DC^{24}), we found that its protective effects against pathogenic IL-17 responses reflect suppression of a cellular network involving DC, Th17, and γδ T cells.[9] Therefore, to address the therapeutic potential of PC-based SMAs of ES-62 in arthritis, we first determined whether a PC-conjugated protein, PC-BSA, could suppress Th1/Th17 responses in CIA. Analysis of its effects (relative to BSA) confirmed and extended our previous findings using PC-ovalbumin (OVA)[8] in that PC-BSA suppressed the severity of disease in terms of articular score (Figure 1A) and hind paw width (Figure 1B) as well as reducing incidence of pathology (Figure 1C), especially that pertaining to high articular score (Figure 1D; score ≥4). Also, as with ES-62, PC-BSA reduced the serum levels of IL-17 (Figure 1E), and this was reflected by reduced percentages and numbers of IL-17-producing $CD4^+$ and γδ T cells stimulated with PMA/ionomycin ex vivo (Figure 1F,H,I). Similarly, and also as observed with ES-62, PC-BSA suppressed IFNγ production by $CD4^+$, $CD8^+$, and γδ T cells (Figure 1G,J−L). Collectively, these data suggested that PC-based SMAs could be a suitable starting point for the development of novel anti-inflammatory drugs for RA.

Molecule Design and Synthesis. Our previous work had shown that PC alone[13,14] and PC esters of short peptides
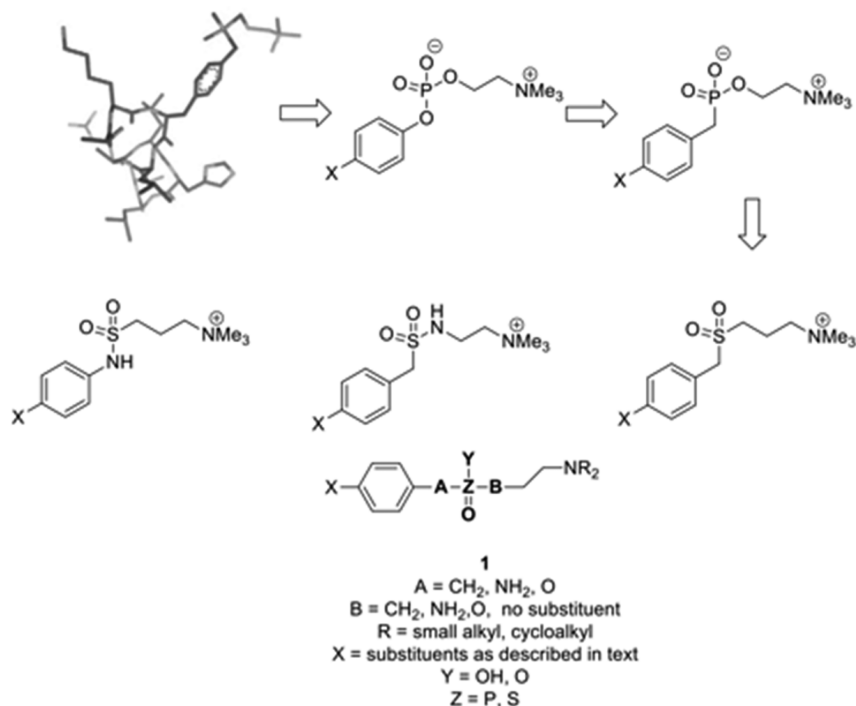
Figure 2. Design of small molecule analogues (SMAs) of ES-62 based upon a tyrosyl-phosphoryl choline peptide.

Scheme 1. Synthesis of Phosphorus-Containing SMAs
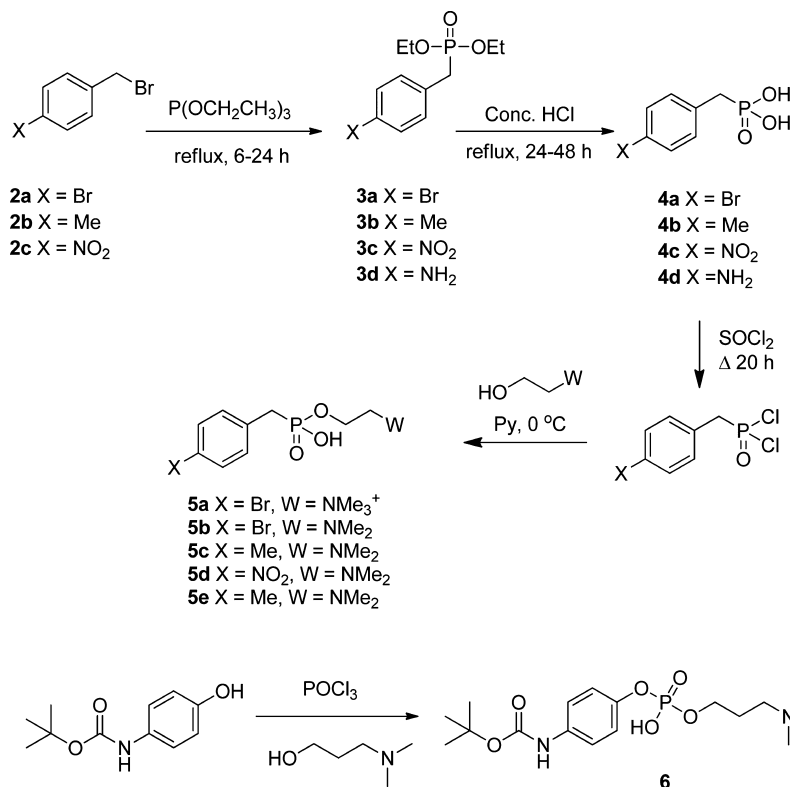
(unpublished results) and lipids[12,15] could reproduce some of the actions of ES-62. However both the size and/or the lability of these compounds suggested that they would not be appropriate as drugs. Moreover, PC esters are known to have a wide range of biological actions, and selectivity would be important for any new drug. A potential solution to these problems is provided by the use of isoesters of the naturally occurring phosphate ester, in which the alkylamino chain and a tetrahedral analogue of the phosphate are included. On the basis of the structure of one of the short peptides, which contained PC-tyrosine, a simple structure was adopted that removed the labile phosphate esters and replaced them with phosphonates, sulfones, sulfonamides, and carboxamides.

Scheme 2. Synthesis of Aminoethylsulfones[a]
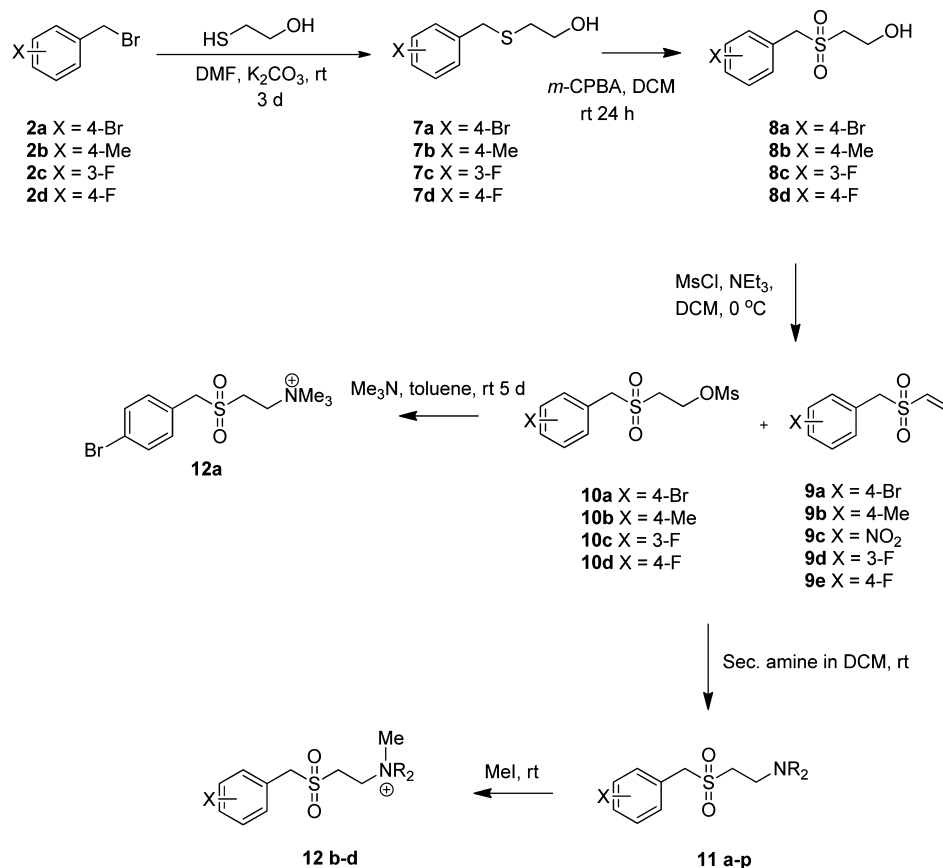
[a]Secondary amines were Me$_2$NH, pyrrolidine, and morpholine. Substituents X and R of compounds evaluated are given in the tables.

Compound Design. The first series of target compounds was the analogous phosphonates. Choline phosphonates, like phosphates, are zwitterionic and likely to have limited cellular penetration. To obtain monocationic small molecule analogues, therefore, the corresponding sulfones and sulfonamides were included. In place of the peptide backbone, small substituents of differing electronic and steric properties were included in the benzene ring, leading to a generic structure (1) in which this substituent, the methylene chain length, and the substituted amino group could be varied (Figure 2).

Sulfones have been used in medicinal chemistry principally in peptidomimetics where they link amino acid-like components to give transition state analogues[25] and activate alkenes to Michael addition in irreversible inhibitors.[26,27] Cathepsin C is an anti-inflammatory target for which vinyl sulfone containing inhibitors have been described.[28] Away from the peptide field, sulfones have featured in inhibitors of terpenoid biosynthesis in farnesyl diphosphate mimetics.[29] It has also been shown that sulfone and sulfonamide analogues of fosmidomycin are inactive compared with the parent compound; in that case, the loss of the negative charge was considered to be significant.[30] The closest structural relatives to the compounds described in this paper can be found in the patent literature, but most are arylsulfones in which the sulfone group is directly attached to the aromatic ring,[31,32] unlike the new compounds described here in which there is a methylene group between aromatic ring and sulfonyl group. Sulfonamides have featured in anti-inflammatory compounds as benzensulfonamides in COX-2 inhibitors,[33] and some recent studies have included N-alkyl or

aryl substituents. Thus the indole-based PLA2 inhibitors[34,35] contain N-alkyl sulfonamides within highly hydrophobic structures. A similar substructure is found in some N-dialkylsulfonamide-containing H4 receptor antagonists.[36]

Synthetic Methods. *Benzylic Halides to Phosphonates to PC Related Derivatives.* Phosphonic acid precursors were prepared from the corresponding benzyl bromides (2a–2c) by the Arbuzov reaction, hydrolysis of the phosphonate esters (3a–3d) to give the corresponding phosphonic acids (3a–3d), activation using thionyl chloride, and finally esterification with choline or an appropriate analogue to give the target compound (Scheme 1, 5a–5e). A phosphate was prepared from the corresponding phenol by phosphorylation with phosphoryl chloride and coupling with choline iodide (Scheme 1, 6).

Benzylic Halides to Alkyl Sulfides Followed by Oxidation to Give Sulfones. Sulfones were prepared from the relevant benzylic halide by alkylation of either 2-thioethanol or 3-thiopropanol followed by oxidation of the thioethers (7a–7d, 13a,b, Schemes 2 and 3, respectively) to give the sulfones (8a–8d, 14a,b). Mesylation in the case of the ethyl derivatives afforded a mixture of the vinyl sulfones (9) and the mesylates (10), which was used without separation to react with the appropriate secondary amine to give a series of the required SMAs (11a–11p, 17a–17f). The exact proportions of the vinyl sulfone and mesylate were typically 70–80% vinyl sulfone depending upon substituent and batch. If the reaction time was 48 h or longer, only vinyl sulfone was obtained. This synthetic step was not optimized because both vinyl sulfone and mesylate afforded the same product under equivalent conditions in the

Scheme 3. Synthesis of Aminopropylsulfones and Phenyl Sulfones[a]
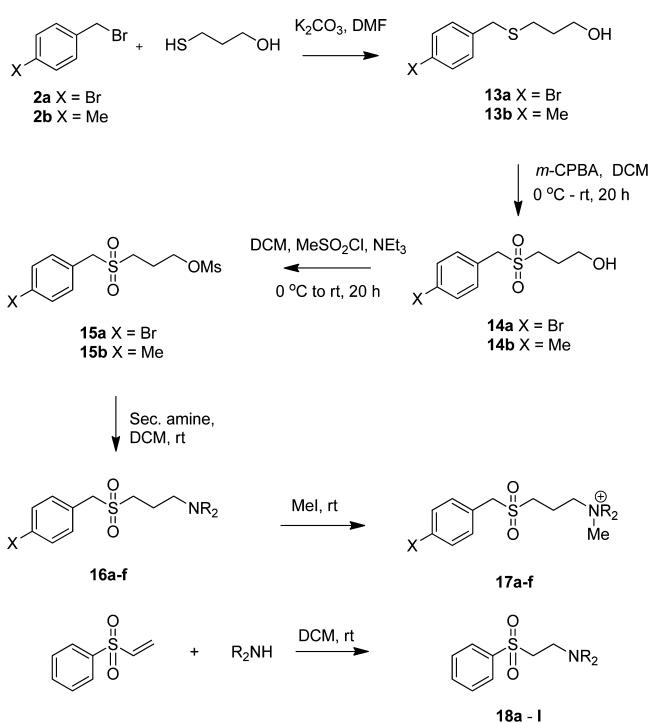
[a]Secondary amines were Me$_2$NH, pyrrolidine, and morpholine. Substituents X and R of compounds evaluated are given in the tables.

following steps. The corresponding quaternary salts (**12b–12d**) were obtained by alkylation with methyl iodide. For the propyl derivatives in which elimination does not occur under mild conditions, substitution of the mesylate directly afforded the required SMAs.

A third series of phenylsulfones (Scheme 3, **18a–18l**) with shorter length than the foregoing compounds was prepared by addition of the appropriate amine to phenylvinylsulfone.

Sulfonamides. Benzyl sulfonamides were simply prepared from the relevant sulfonyl chloride and amine under standard conditions (Scheme 4, **19a–19aa**). Arylamino sulfonamides (**21a–21p**) were prepared from the vinyl sulfonamide (**20a–20e**) of the appropriate aniline or benzylamine.

Carboxamides (**24a–24d**, **25a–25d**) were prepared by acylation of the appropriate amine with the acid chloride in dichloromethane solution (Scheme 5). The isoquinolylmethyl-lamide (**24e**) was prepared by HBTU coupling of the amine and sodium 3-(4-morpholinyl)propanoate.

Screening of SMAs. A single screen of a library of 116 novel compounds was carried out for modulation of production of the Th1/Th17 promoting inflammatory cytokines IL-12p40 and IL-6 by bone marrow-derived macrophages (bmMs) in response to the PAMPs, LPS (TLR4), bacterial lipoprotein (BLP, TLR2/6), and CpG motifs (TLR9), to identify SMAs that mimicked the properties of ES-62 (Table 1).[4,37,38] Previously, we had successfully tested PC,[14] PC-peptides (unpublished), and PC-lipids[12,15] in the concentration range 1–10 μg/mL for analysis of effects on cytokine production in vitro, and so a concentration of 5 μg/mL was selected for the current study. Activity at such a concentration would reflect a significant reduction in potency relative to ES-62 (active at 1–2 μg/mL[38]), which has PC probably accounting for <1% of its mass.[39,40] This could possibly be due to the structure of ES-62

and/or its mechanism of interaction with cells, somehow optimizing PC presentation and/or activity.

Many of the compounds were found to demonstrate immunomodulatory activity. However, perhaps unexpectedly, they were selective in terms of the PAMP and/or cytokine responses they affected and, indeed, in some cases cytokine levels were elevated rather than reduced, a result not previously observed with ES-62. Nevertheless, a number of trends are detectable from the cytokine release data.

In general, the tail group structure had no detectable influence on the cytokine release profile although a significant effect of the diamino tail group was observed for **21p** and **21q** as noted below. Although severely limited by the range of aromatic substituents studied, there was a notable difference between the reduction of pro-inflammatory cytokine release (4-Br and 4-Me **11a–11d**) and the tendency to show a lack of an effect or even an increase in pro-inflammatory cytokine release (3-F **11e–11h**).

In the sulfone series, compounds with a two-carbon methylene chain (**11a–11p** and **12a–12d**) were generally more effective than comparable compounds with a three-carbon methylene chain (**16a–16f** and **17a–17e**) at inhibiting pro-inflammatory cytokine release. Shortening the distance between the aromatic ring and the amine essentially increased pro-inflammatory cytokine release (**18a–18l**), but some reduction of cytokine release was observed, suggesting that there are different targets and mechanisms for these compounds in differently stimulated cells.

The cytokine release signature of many of the sulfonamides was to stimulate the release of pro-inflammatory cytokines (CSN type **19d–19j**, CNS type **21c–21i**), and as with the sulfones, there was no evidence for an effect caused by the side chain structure. However there were two subsets of sulfonamides that caused predominant reduction in the release of pro-inflammatory cytokines; in the CNS type, compounds with electron withdrawing substituents (F, NO$_2$ **21l–21o**) or both CNS and CSN types with large hydrophobic aromatic groups (naphthyl, **19u**, 'coumarinyl', **21r–21t**).

A further special case of reduced pro-inflammatory cytokine release was found for compounds of the CNS type with the dimethylaminoethylamino tail group (**21p**, **21q**) for which some monoamino analogues had the opposite effect (**21e**, **21f**, **21h**).

The shortened NSC type of sulfonamide (**23a–23h**) responded with a decrease in release of IL-12p40 in LPS stimulated cells but an increase in IL-6 release from CpG stimulated cells, again largely independent of tail group structure.

The amides (**24a–24c**, **25a–25d**) almost entirely caused a reduction in the release of pro-inflammatory cytokines.

Most strikingly, the phosphate and phosphonates, all of which are zwitterionic, in general caused an increase in pro-inflammatory cytokine release, suggesting that a distinctly different mechanism was stimulated by these compounds from that of the nonzwitterionic sulfones, sulfonamides, and amides.

Selection of Compound for in Vivo Evaluation. Of direct relevance to the aims of the project, a number of the compounds reduced production of cytokines important for promoting Th1 and/or Th17 responses, IL-12p40 and/or IL-6, in response to one or more of the TLR ligands. However, some of these did not target either TLR4 (sulfonamide **21o**) or TLR2 (sulfonamides **21n**, **21o**) responses. Likewise, of the carboxamides, **24c** only effectively targeted both CpG

Scheme 4. Synthesis of Sulfonamides[a]
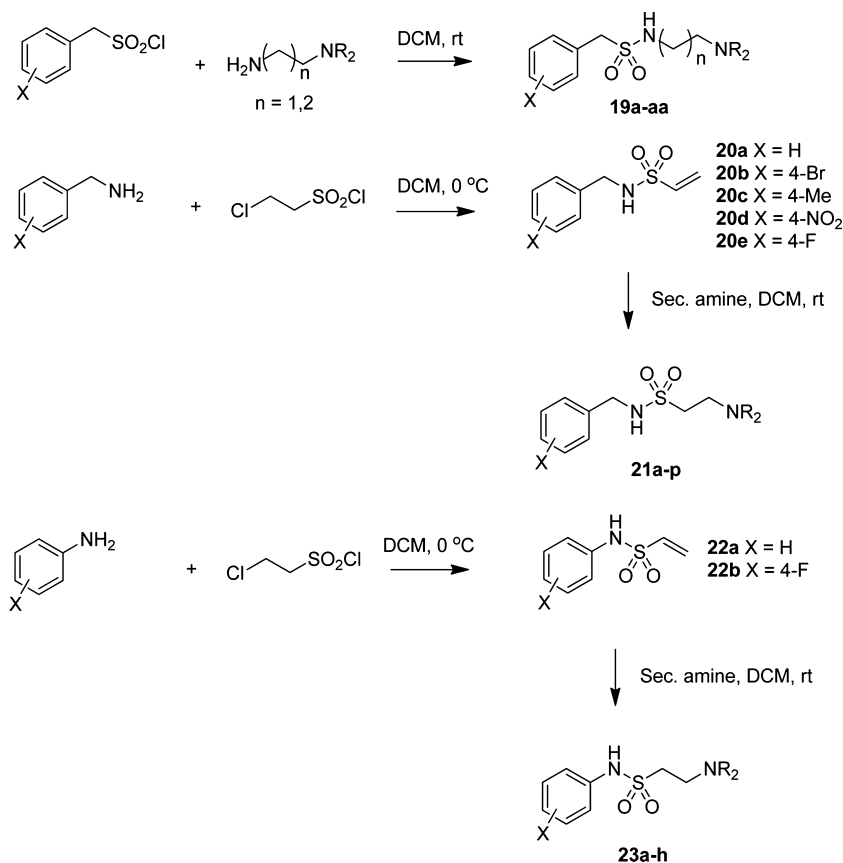
[a]Substituents X and R of compounds evaluated are given in the tables. (**19**) is referred to as the CSN type, (**21**) as the CNS type, and (**23**) as the NSC type in the text.

Scheme 5. Synthesis of Carboxamides[a]
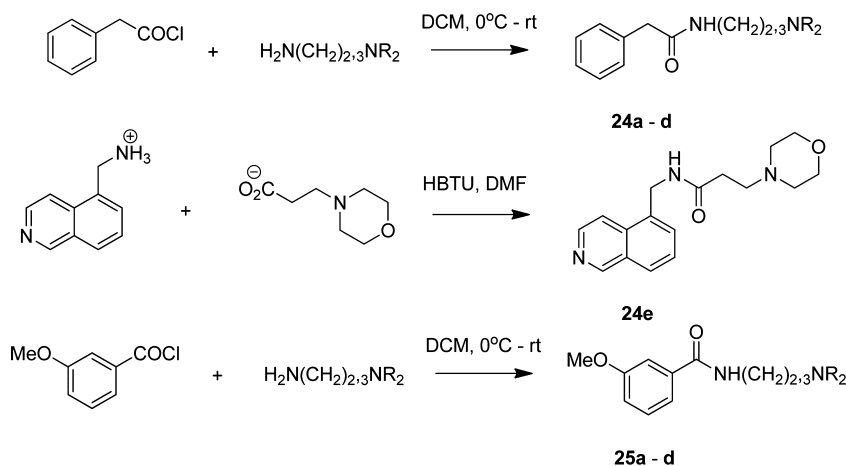
[a]Substituents X and R of compounds evaluated are given in the tables.

responses. The most promising compounds were those that showed the broadest response to the PAMPs, the sulfones, **11a** and **12b**, the sulfonamide **21l**, and the carboxamide **24b**. **11a** (see Figure 3A) and **12b** both mimicked ES-62 in targeting IL-12p40 production via each of TLR2, 4, and 9, and this cytokine is pathogenic in CIA[41] due to it being a component of both IL-12p70 and IL-23, which promote Th1 and Th17 responses, respectively, and hence a therapeutic target (ustekinumab) in inflammatory autoimmune diseases.[42,43] By contrast, sulfona-

mide **21l** and carboxamide **24b** did not target LPS- and BLP-mediated IL-12p40 responses, respectively. Sulfone **11a** additionally targeted IL-6 production (see also Figure 3B) in response to all three TLRs (although this did not reach statistical significance for TLR2 in all experiments), and this cytokine has also been shown to be pathogenic[44] and thus a therapeutic target (tocilizumab) in RA.[45] Although sulfone **12b** could suppress CpG-mediated IL-6 responses, it was less effective at inhibiting such TLR2- or TLR4-coupled responses

Table 1. Modulatory Effect of the Library of Small Molecule Analogues on TLR-Dependent Cytokine Production[a]

$$\text{[generic scaffold: benzene ring bearing } Y \text{; } X\!-\!(\,)_n\!-\!Z \text{ chain]}$$
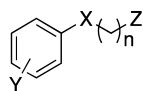
(A) phosphonates and phosphates

SMA	X	Y	n	Z	LPS IL-12	LPS IL-6	BLP IL-12	BLP IL-6	CPG IL-12	CPG IL-6
5a	$CH_2PO_3^-$	4-Br	2	NMe_3^+	↓	↑	↓			
5b	$CH_2PO_3^-$	4-Br	2	NMe_2		↑				↑
5c	$CH_2PO_3^-$	4-Me	2	NMe_2	↑					
5d	$CH_2PO_3^-$	4-NO_2	2	NMe_3^+	↑	↑				
5e	$CH_2PO_3^-$	4-Me	2	NMe_2	↑		↑			
6	OPO_3^-	4-BOCNH	3	NMe_2		↑				↑

(B) sulfones

SMA	X	Y	n	Z	LPS IL-12	LPS IL-6	BLP IL-12	BLP IL-6	CpG IL-12	CpG IL-6
11a	CH_2SO_2	4-Br	2	Me_2N	↓	↓	↓		↓	↓
11b	CH_2SO_2	4-Me	2	Me_2N	↓	↓				
11c	CH_2SO_2	4-Me	2	pyrrol	↓	↓	↓	↓		
11d	CH_2SO_2	4-Br	2	pyrrol	↓					
11e	CH_2SO_2	3-F	2	NMe_2	↑	↑				
11f	CH_2SO_2	3-F	2	diam						
11g	CH_2SO_2	3-F	2	morph			↑			
11h	CH_2SO_2	3-F	2	pyrrol			↑	↓		
11i	CH_2SO_2	4-F	2	NMe_2			↓	↓		
11j	CH_2SO_2	4-F	2	morph			↓	↑	↑	
11k	CH_2SO_2	4-F	2	pyrrol	↑		↓			
11l	CH_2SO_2	4-F	2	diam			↓			
11m	CH_2SO_2	3-F	2	S-2-Me-but						
11n	CH_2SO_2	3-F	2	R-2-Me-but			↓	↓		
11o	CH_2SO_2	4-Br	2	S-2-Me-but			↓			
11p	CH_2SO_2	4-Br	2	R-2-Me-but						
12a	CH_2SO_2	4-Br	2	Me_3N^+						
12b	CH_2SO_2	4-Me	2	Me_3N^+	↓		↓		↓	↓
12c	CH_2SO_2	4-Me	2	pyrrol Me⁺	↓		↓			
12d	CH_2SO_2	4-Br	2	pyrrol Me⁺	↓	↓	↓			
16a	CH_2SO_2	4-Br	3	pyrrol						
16b	CH_2SO_2	4-Br	3	NMe_2		↓				
16c	CH_2SO_2	4-Br	3	morph			↑	↓		
16d	CH_2SO_2	4-Me	3	pyrrol						
16e	CH_2SO_2	4-Me	3	NMe_2						
16f	CH_2SO_2	4-Me	3	morph						
17a	CH_2SO_2	4-Br	3	morph Me⁺			↑			
17b	CH_2SO_2	4-Br	3	Me_3N^+		↓		↓		
17c	CH_2SO_2	4-Br	3	pyrrol Me⁺						
17d	CH_2SO_2	4-Me	3	pyrrol Me⁺						
17e	CH_2SO_2	4-Me	3	Me_3N^+						
18a	SO_2	H	2	diam					↑	
18b	SO_2	H	2	thiomorph	↓	↓			↑	
18c	SO_2	H	2	morph			↑	↓		
18d	SO_2	H	2	pyrrol			↑	↓		
18e	SO_2	H	2	R-2-Me-but	↑	↑				
18f	SO_2	H	2	S-2-Me-but						
18g	SO_2	H	2	diam (−Me)						
18h	SO_2	H	2	n-Pr	↑	↑	↓	↓		
18i	SO_2	H	2	i-Pr			↓			
18j	SO_2	H	2	3-OH-n-Pr	↑	↑	↓			
18k	SO_2	H	2	t-Bu			↑	↓		
18l	SO_2	H	2	4-Me-pip						

(C) sulfonamides and carboxamides

SMA	X	Y	n	Z	LPS IL-12	LPS IL-6	BLP IL-12	BLP IL-6	CpG IL-12	CpG IL-6
19a	CH_2SO_2NH	H	2	NMe_2					↑	
19b	CH_2SO_2NH	H	2	pyrrol						

Table 1. continued

					(C) sulfonamides and carboxamides					
SMA	X	Y	n	Z	LPS IL-12	LPS IL-6	BLP IL-12	BLP IL-6	CpG IL-12	CpG IL-6
19c	CH_2SO_2NH	H	2	morph						
19e	CH_2SO_2NH	4-Br	2	NMe_2			↑		↑	
19d	CH_2SO_2NH	4-Br	2	pyrrol					↑	
19f	CH_2SO_2NH	4-Br	2	morph					↑	↑
19g	CH_2SO_2NH	4-F	2	NMe_2					↑	↑
19h	CH_2SO_2NH	4-F	2	pyrrol	↑		↑		↑	↑
19i	CH_2SO_2NH	4-F	2	morph					↑	↑
19j	CH_2SO_2NH	4-Me	2	NMe_2	↑					
19k	CH_2SO_2NH	4-Me	2	pyrrol						
19l	CH_2SO_2NH	4-Me	2	morph						
19m	CH_2SO_2NH	4-NO_2	2	NMe_2				↓		
19n	CH_2SO_2NH	4-NO_2	2	pyrrol						
19o	CH_2SO_2NH	4-NO_2	2	morph						
19p	CH_2SO_2NH	4-Br	3	NMe_2						
19q	CH_2SO_2NH	4-NO_2	3	NMe_2				↓		
19r	CH_2SO_2NH	4-Me	3	NMe_2						
19s	CH_2SO_2NH	4-F	3	NMe_2						
19t	CH_2SO_2NH	H	3	NMe_2	↑					
19u	CH_2SO_2NH	2-naphthyl	2	morph		↓	↓		↓	↓
19v	CH_2SO_2NH	2-naphthyl	2	pyrrol					↓	
19w	CH_2SO_2NH	2-naphthyl	2	NMe_2						
19x	CH_2SO_2NH	4-stilbenyl	2	NMe_2			↓			
21a	CH_2NHSO_2	H	2	pyrrol						
21b	CH_2NHSO_2	H	2	morph						
21c	CH_2NHSO_2	H	2	NMe_2				↑		
21d	CH_2NHSO_2	4-Br	2	morph						
21e	CH_2NHSO_2	4-Br	2	pyrrol	↑	↑	↑	↑		
21f	CH_2NHSO_2	4-Br	2	NMe_2						↑
21g	CH_2NHSO_2	4-Me	2	morph						
21h	CH_2NHSO_2	4-Me	2	pyrrol		↑		↑		↑
21i	CH_2NHSO_2	4-Me	2	NMe_2				↑		↑
21j	CH_2NHSO_2	4-NO_2	2	morph						
21k	CH_2NHSO_2	4-NO_2	2	pyrrol						
21l	CH_2NHSO_2	4-NO_2	2	NMe_2		↓	↓	↓	↓	↓
21m	CH_2NHSO_2	4-F	2	morph		↓		↓	↓	↓
21n	CH_2NHSO_2	4-F	2	pyrrol		↓			↓	↓
21o	CH_2NHSO_2	4-F	2	NMe_2					↓	
21p	CH_2NHSO_2	4-Me	2	diam	↓	↓		↓		↓
21q	CH_2NHSO_2	4-Br	2	diam	↓			↓	↓	
21r	CH_2SO_2NH	'coumarin'	2	morph	↓		↓			
21s	CH_2SO_2NH	'coumarin'	2	pyrrol	↓		↓			
21t	CH_2SO_2NH	'coumarin'	2	NMe_2	↓		↓			
23a	$NHSO_2$	H	2	NMe_2	↓					
23b	$NHSO_2$	H	2	pyrrol	↓				↓	
23c	$NHSO_2$	H	2	morph						
23d	$NHSO_2$	4-F	2	NMe_2	↓					↑
23e	$NHSO_2$	4-F	2	pyrrol	↓					
23f	$NHSO_2$	4-F	2	morph	↓					↑
23g	$NHSO_2$	4-F	2	diam	↓					↑
23h	$NHSO_2$	H	2	diam	↓					↑
24a	CH_2CONH	H	2	NMe_2	↓					↓
24b	CH_2CONH	H	2	pyrrol	↓	↓		↓	↓	↓
24c	CH_2CONH	H	2	morph	↓				↓	↓
24d	CH_2CONH	H	3	NMe_2						
24e	CH_2NHCO	5-isoquinolyl	2	morph				↓		
25a	CONH	3-MeO-C_6H_4	2	NMe_2	↓	↓				↓
25b	CONH	3-MeO-C_6H_4	2	pyrrol	↓	↓				↓
25c	CONH	3-MeO-C_6H_4	2	Morph	↓	↓				↓
25d	CONH	3-MeO-C_6H_4	3	NMe_2	↓			↑		↓

Table 1. continued

[a]Bone marrow-derived macrophages preincubated for 18 h with 5 μg/mL of compounds were stimulated with 100 ng/mL LPS, 10 ng/mL BLP, or 0.01 μM CpG in the continued presence of the compounds. After 24 h, supernatants were collected and measured for their IL-12p40 and IL-6 content by ELISA. Arrows down (↓) indicate statistically significant (at least $p < 0.05$) down-regulation and arrows up (↑) statistically significant up-regulation of the levels of cytokine versus control; blank squares = no significant change. Abbreviations used in structural formulas: 'coumarin' = (7-methoxy-2-oxo-2H-chromen-4-yl)methyl; diam = N,N,N-1,1,2-tetramethylethylenediamino2-Me-but = 2-methylbutylamino; 4-Me-pip = 4-methylpiperazinyl; morph = morpholino; 3-OH-n-propyl = 3-hydroxypropylamino; pyrrol = pyrrolidino; stilbenyl = 1-(4-[(E)-2-phenylethyl]benzyl; thiomorph = thiomorpholino.
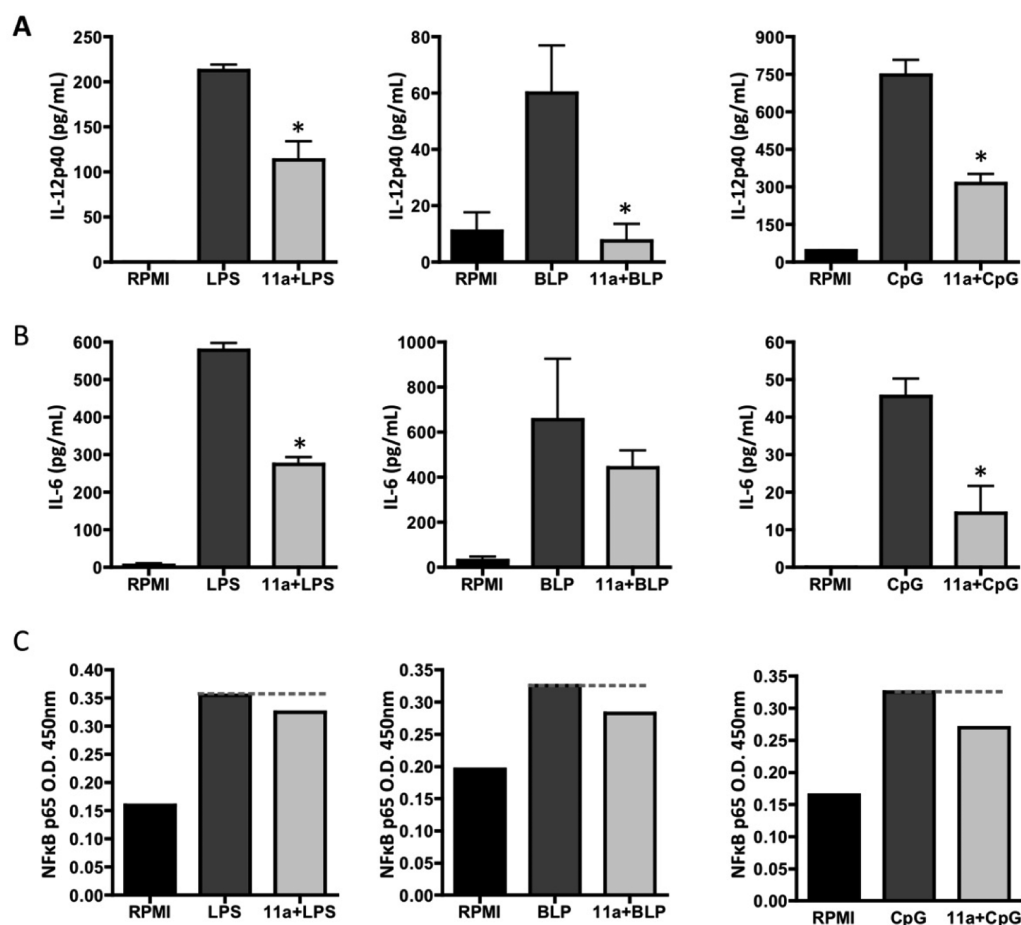
Figure 3. 11a-related changes in macrophage cytokine production and signaling of p65 NFκB in response to LPS, BLP, and CpG. BmMs were preincubated with 11a at 5 μg/mL for 18 h prior to stimulation with 100 ng/mL LPS, 10 ng/mL BLP, or 0.01 μM CpG for 24 h and analysis of levels of IL-12p40 (A) and IL-6 (B) performed by ELISA. (C) Stimulation with PAMPs as above for LPS and BLP, and 1 μM CpG, but for 1 h and the level of p65 activation in duplicate samples measured by TransAM. For statistical analysis for (A) and (B), *$p < 0.05$.

(decreases not reaching statistical significance), which have been shown to be important in the development of inflammatory Th17 responses, including those in arthritis.[46−48] Moreover, as observed with ES-62,[40,49] (11a (Figure 3C), but not 21l (results not shown), was able to inhibit TLR-mediated p65 NF-κB activation in response to all three PAMPs.

Thus, as both IL-6 and IL-12p40 (via IL-23) promote the differentiation and maintenance of Th17 responses, it was considered that 11a was most likely to mimic the protective effects of ES-62 in CIA by suppressing production of IL-17,[9] a cytokine that is pathogenic in RA and an emerging therapeutic target (for example via the humanized monoclonal antibody LY2439821 and the human monoclonal antibody AIN457; reviews refs 42,50−52). Limited analysis of potency revealed that 11a was still able to induce a statistically significant reduction of LPS-stimulated production of IL-6 by macrophages when the concentration was reduced to 1 μg/mL, but

significant effects were not consistently observed at 0.2 μg/mL (data not shown). Like ES-62, 11a showed no evidence of toxicity under conditions mimicking the macrophage screen of cytokine production as determined using the cell viability indicator, 7-actinomycin D (7-AAD) (Figure 4). Indeed, the SMA showed some evidence of protecting against the loss of cell viability associated with exposure to LPS. 11a was thus considered suitable for testing in vivo.

In Vivo Evaluation: 11a Protects against Collagen-Induced Arthritis. 11a, at a low dose of ∼50 μg/kg per injection, was tested in the CIA model and it was found that, as with ES-62, it effectively reduced development of arthritis in treated mice. This was reflected in each of disease scores (Figure 5A), hind paw width (Figure 5B), disease incidence (Figure 5C), and percentage of mice with high disease scores (Figure 5D). Moreover, whereas mice with CIA exhibited a significant increase in DLN cell number over the control group
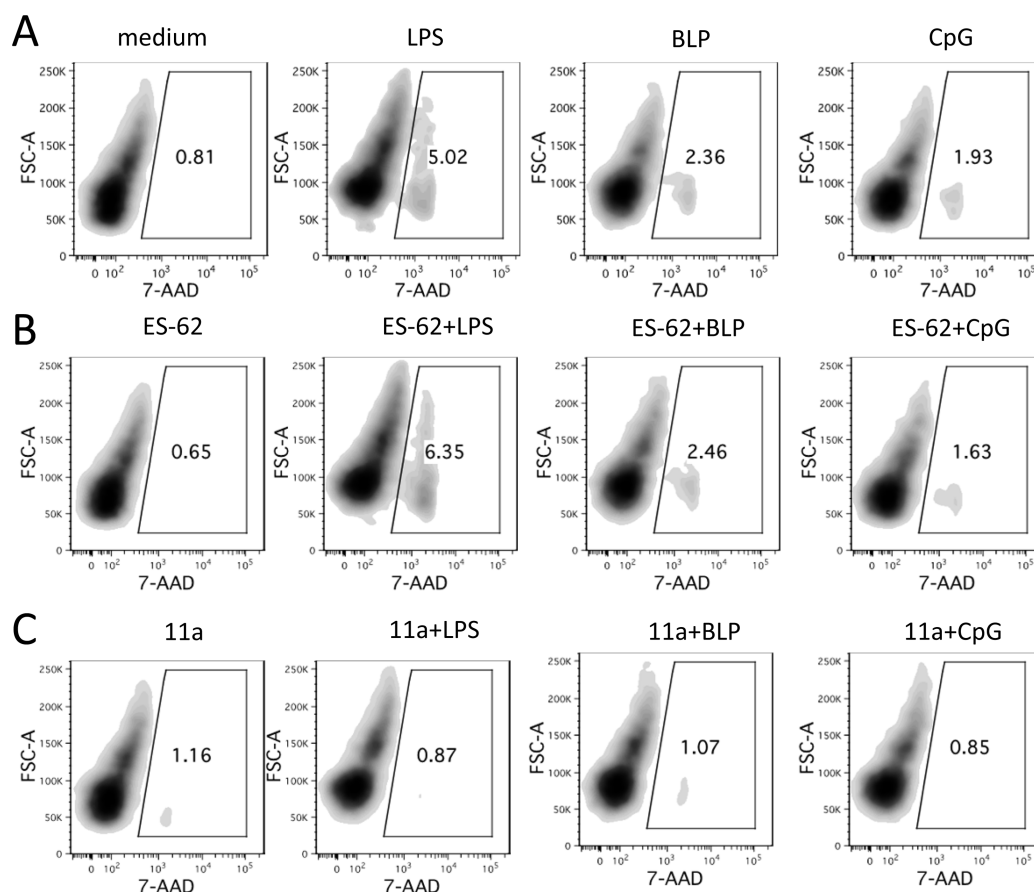
Figure 4. Lack of toxic effect of **11a** on macrophages. BmMs in ultralow binding tissue culture plates were rested in RPMI complete medium for 24 h before culturing with fresh medium or medium containing **11a** (5 μg/mL) or ES-62 (2 μg/mL). After 18 h, the macrophages were stimulated with medium containing 100 ng/mL LPS or 10 ng/mL BLP or 0.01 μM CpG for an additional 24 h before staining with 7-AAD to assess their viability. The samples were analyzed by flow cytometry, and the data are presented as density plots with frequency of 7-AAD positive (dead) cells indicated in the gates. The results shown are from a single experiment representative of two independent experiments.

not exposed to collagen, this was significantly reduced by treatment with **11a** (Figure 5E) and to a level not significantly different from the control naive group. This result was mirrored by analysis of defined T cell populations, namely CD4^{+} T cells (Figure 5F), CD8^{+} T cells (Figure 5G), and $\gamma\delta$ T cells (Figure 5H), where **11a**-treated mice showed reduced levels of cells relative to mice with CIA and/or levels not significantly different to the control group of naive mice not exposed to collagen. Previously we had found that CD4^{+} and $\gamma\delta$ T cells from ES-62-treated mice were similarly reduced, although statistical significance had not been reached.[9]

11a Protection against CIA Correlates with Suppression of IFNγ and IL-17 Responses. Our previous work with ES-62 showed that it suppressed both IFNγ and IL-17 responses[7,9] and hence we investigated whether this was also the case for **11a**. Indeed, similarly to ES-62, we found **11a** to target IFNγ (Figure 6A) and IL-17 (Figure 6B) responses in DLN cells stimulated with PMA/ionomycin ex vivo. First, whereas mice with CIA displayed significantly higher numbers of DLN, CD8^{+} T, and CD4^{+} T cells producing IFNγ in response to PMA/ionomycin-stimulation than naïve mice, this was not true of the **11a**-treated mice exposed to collagen. Moreover, the numbers of IFNγ-expressing cells in the DLN and CD8^{+} T cell populations were significantly reduced in the **11a** group relative to the PBS-CIA group (Figure 6A). However, no significant difference in IFNγ-producing $\gamma\delta$ T

cells was found between the mice exposed to collagen given **11a** or not (results not shown). With respect to IL-17, the effects observed were not as striking although it was still possible to see clear evidence that this pro-inflammatory cytokine was also being targeted. Thus, for example, the numbers of DLN, CD4^{+}, and $\gamma\delta$ T cells were significantly higher in PBS, but not **11a**, treated mice undergoing CIA than in mice not exposed to collagen (Figure 6B).

Unlike in our earlier study with ES-62,[9] **11a** did not induce a statistically significant reduction in the serum levels of IL-17 in these mice (Figure 7A). However, in our previous study,[9] it was shown that pre-exposure to ES-62 inhibited the capacity of dendritic cells (bmDCs) to respond to LPS by secretion of the pro-inflammatory cytokine TNF-α and two cytokines, IL-6 and IL-23, associated with polarization and maintenance of Th17 cells, respectively, and when these experiments were repeated with the bmDCs pre-exposed to **11a**, production of all three cytokines was significantly reduced (Figure 7B). As with ES-62,[4] this did not reflect downregulation of TLR4 expression or reduction in bmDC viability (data not shown). Furthermore, consistent with the ability of **11a** to inhibit production of the two Th17-promoting cytokines, **11a**-treated DCs demonstrate a reduced ability to drive naïve antigen (OVA)-specific Th cells toward a Th17 phenotype, as evidenced by suppression of OVA-specific IL-17 production in such bmDC-CD4^{+} T cell
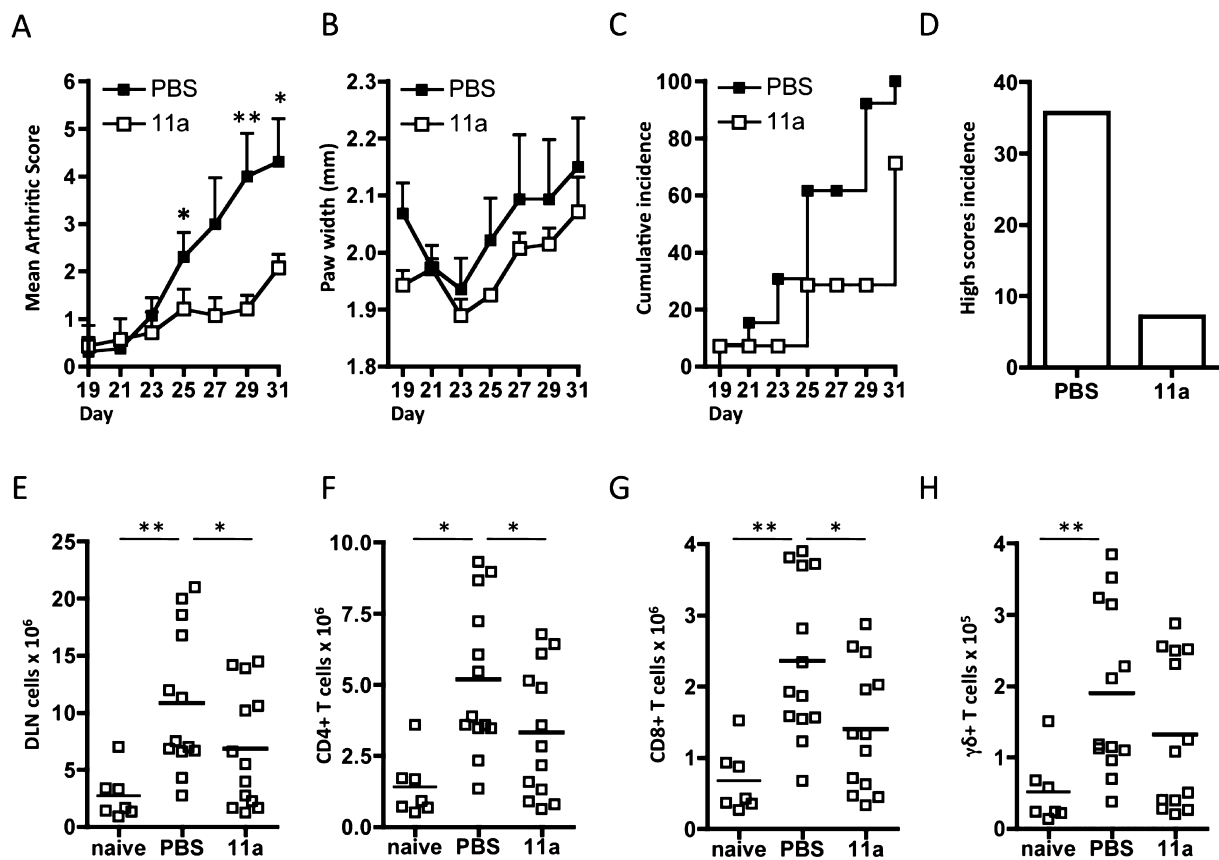
Figure 5. 11a protects against CIA. Disease is shown by each of mean arthritis score ((A) PBS, $n = 13$; **11a**, $n = 13$, data pooled from two independent experiments), hind paw width ((B) $n = 7$, data from a single experiment), and incidence (C,D) indicated by the % of mice developing a severity score ≥ 2 ((C) cumulative incidence) or ≥ 4 ((D) high score incidence). Results are expressed as mean scores $\pm$ SEM for PBS or **11a**-treatment groups of mice exposed to collagen. The numbers of each of total (E), CD4$^+$ (F), CD8$^+$ (G), and $\gamma\delta$ (H) T cells in DLN of individual mice from the naïve ($n = 7$), PBS-treated ($n = 13$) and **11a**-treated ($n = 13$) groups are shown. For statistical analysis, *$p < 0.05$ and **$p < 0.01$.
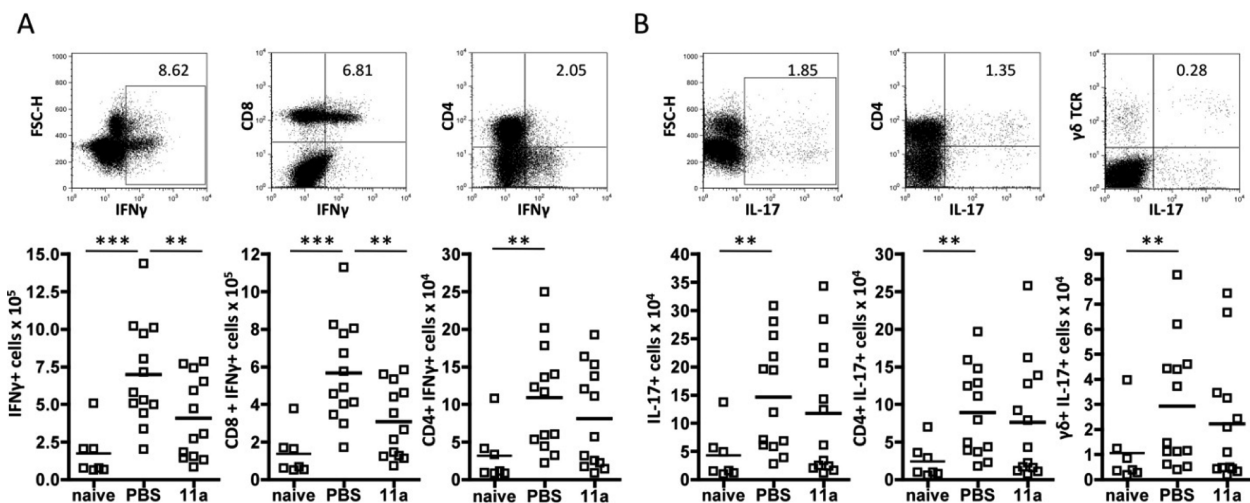
Figure 6. 11a suppresses IFNγ and IL-17 responses in CIA. Exemplar plots of gating strategy of intracellular IFNγ (A) and IL-17 (B) expression by DLN cells from representative individual PBS-treated mice with CIA show forward scatter (FSC) or CD4, CD8, and $\gamma\delta$ expression on the y-axis versus cytokine expression on the x-axis as indicated. The number of (A) IFNγ-expressing total DLN cells, CD8$^+$ T cells, and CD4$^+$ T cells and (B) IL-17-expressing total DLN cells, CD4$^+$ T cells, and $\gamma\delta$ T cells following stimulation with PMA/ionomycin from individual mice are shown (naïve, $n = 7$; PBS, $n = 13$; **11a**, $n = 13$). For statistical analysis, **$p < 0.01$ and ***$p < 0.001$.

cocultures (Figure 7C,D). Again, this is consistent with what was previously observed with ES-62.[9]

11a Is Able to Cause Downregulation of the TLR Signaling Adaptor Myeloid Differentiation Primary

Response Gene 88 (MyD88). Previous work published by our group has shown that ES-62's mechanism of action involves downregulation of the key TLR/IL-1R signaling adaptor MyD88 in Th17 cells[9] and mast cells.[53] This is also true of
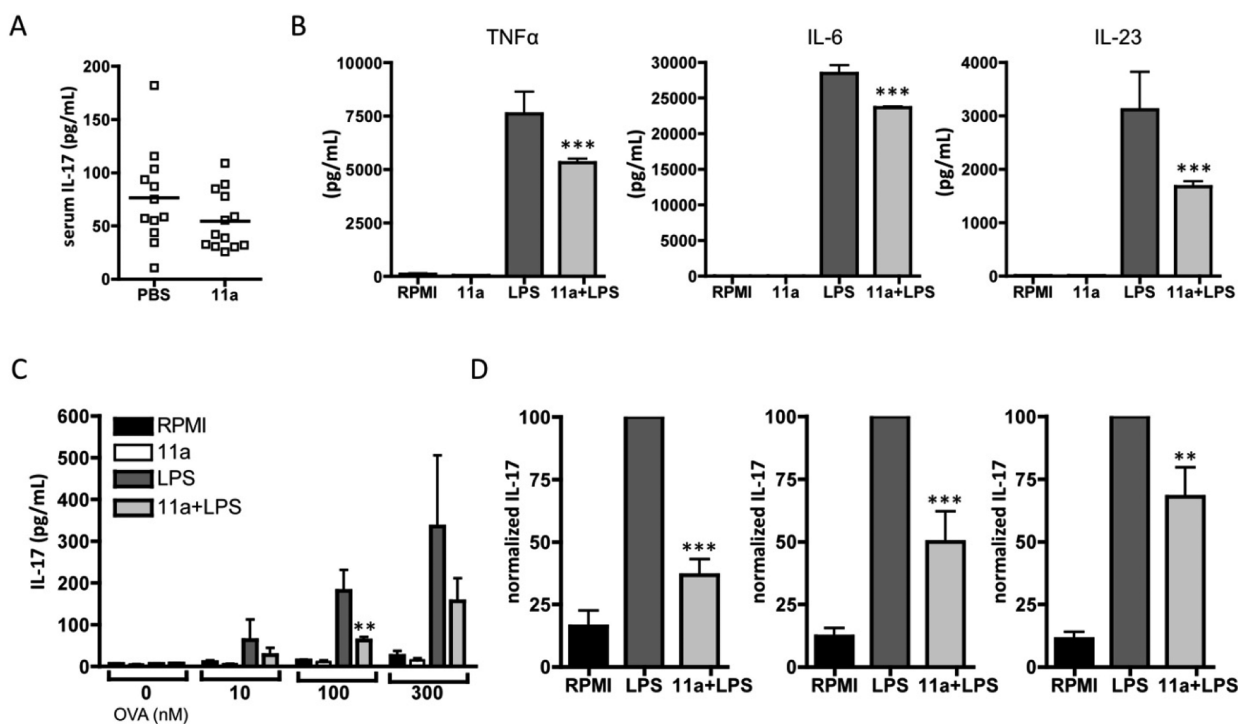
Figure 7. 11a inhibits Th17 polarization. (A) Serum IL-17 levels are plotted as mean values of triplicate IL-17 analyses from individual mice (PBS, n = 12; **11a**, n = 13). (B) BmDCs from C57BL/6 mice were preincubated with or without (**11a**) (5 µg/mL) for 2 h prior to stimulation with LPS for 24 h, and TNFα, IL-6, and IL-23 levels were then analyzed. Data are the mean values (of triplicate samples) ± SEM pooled from 4 independent experiments. (C) BmDCs from BALB/c mice preincubated with or without **11a** (5 µg/mL) were pulsed with the indicated concentration of OVA peptide and cocultured with naive OVA-specific CD4$^+$ T cells (DO.11.10/BALB/c) for 3 days before measuring IL-17 release. Data are the mean values ± SD of duplicate samples pooled from two independent experiments (n = 4). (D) Pooled normalized data from four independent experiments analyzing the effect of **11a** on IL-17 release from bmDC (C57BL/6)-OVA-specific CD4$^+$T cell (OT-II/C57BL/6) cocultures. Data are presented as the means of the mean percentage maximum (LPS) response ± SEM where data were normalized to the LPS response at 10 nM (left), 100 nM (middle), and 300 nM (right) OVA, respectively. * $P < 0.05$; ** $P < 0.01$; *** $P < 0.001$.

macrophages (our unpublished results), the cell type used for our primary screen, and so we next investigated whether **11a** was also able to cause downregulation of MyD88 in these cells. As shown in Figure 8A,B, the SMA does indeed cause significant downregulation of the signaling adaptor in these cells. Figure 8A−C also shows that, as expected, LPS causes an increase in MyD88 expression within the cells, but as demonstrated in Figure 8C, this is prevented by **11a**. A simple schematic of the proposed mechanism of action of **11a** is shown in Figure 8D and described in detail in the figure legend.

■ **DISCUSSION AND CONCLUSIONS**

The increasing awareness of the therapeutic potential of parasitic worms has resulted in a search to identify defined molecules that possess immunomodulatory properties and recently details of a number of these have appeared.[11] Although some of the molecules characterized to date are carbohydrate[56] or lipid[57] in nature, the majority are proteins, and hence there is the potential problem of their immunogenicity possibly interfering with activity. ES-62, which is among the best characterized of helminth-derived immunomodulators,[58] is active in mouse models of both allergic and autoimmune diseases[58] and has been suggested as being the helminth-derived molecule for which there is most potential in testing in humans for treatment of such disorders.[59] Furthermore, PC-containing molecules circulate in the bloodstream of humans infected with filarial nematodes for decades without inducing any known adverse effects on general health or compromising

the capacity to fight infection, therefore suggesting that ES-62 might be safer than current immunosuppressive drugs, including glucocorticoids or biologics, used to treat human inflammatory diseases. However, as a large protein, ES-62 is subject to the problem of immunogenicity referred to above and hence in reality is not suitable for use as a drug. Nevertheless, our data obtained to date indicated that PC is the key anti-inflammatory moiety of ES-62,[5,8,10,11] and this was confirmed in the present study as when conjugated to BSA, it was found to mimic the suppressive effects of ES-62 on IL-17 and IFNγ responses. Hence we decided to pursue a novel strategy of drug development: designing synthetic small drug-like compounds based around PC.

The SMA library was initially subjected to a simple in vitro screen that involved determining the effect of the compounds on PAMP-induced macrophage pro-inflammatory cytokine responses, in particular focusing on those mediators that might contribute to Th1/Th17 responses, which are known targets of ES-62 in CIA.[9] The results of this screen were surprising, in that although a number of the SMAs targeted macrophage responses, the effects were more selective than those recorded previously with ES-62, in the sense that not all PAMP-induced cytokine responses were inhibited. Although unexpected, these may actually be potentially important observations, raising the possibility of generating drugs more specific than ES-62 with respect to anti-inflammatory activity. Another unexpected finding was that rather than inhibiting the cytokine responses, a number of the SMAs increased certain
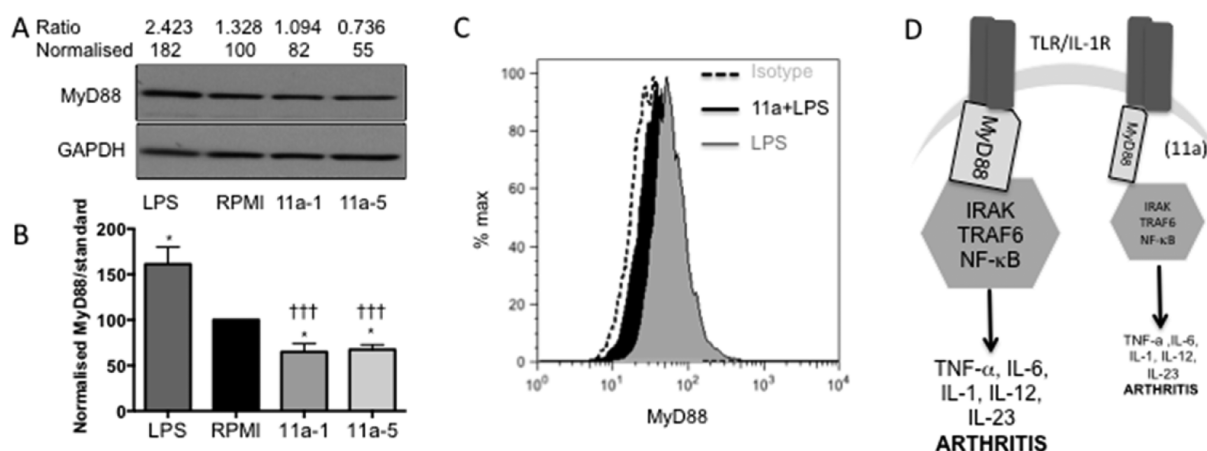
Figure 8. **11a** downregulates MyD88 expression in macrophages. (A) BmMs treated with medium (RPMI), **11a** at 1 and 5 μg/mL (**11a-1** or **11a-5**), or LPS (100 ng/mL) for 20 h were analyzed by Western blotting for expression of MyD88 and loading control GAPDH. Levels of expression were determined by densitometry using Image-J software and expressed as the ratio of MyD88:GAPDH and normalized to the RPMI value. (B) Data from six analyses revealed that while LPS significantly increased MyD88 expression (*$p < 0.05$), both **11a-1** and **11a-5** reduced it (*$p < 0.05$) relative to the RPMI control. In addition, the level of MyD88 in cells treated with either **11a-1** or **11a-5** was significantly different ([†††]$p < 0.001$) to that in those exposed to LPS. (C) Flow cytometric analysis of MyD88 expression in permeabilised bmMs relative to isotype control (20,000 bmMs/treatment group). BmMs were treated with RPMI or **11a** (at 5 μg/mL) for 2 h prior to exposure to LPS (100 ng/mL) for a further 18 h, and consistent with the Western blot data, LPS upregulated levels of MyD88 (127% relative to MFI of RPMI-treated bmMs). Moreover, bmMs pretreated with **11a** exhibited lower levels of MyD88 expression (MFI for **11a** + LPS is 95.7% of the level of the RPMI value: the RPMI trace is not shown due to its overlap with that of **11a** + LPS) than cells treated with LPS alone. (D) Simple schematic of model of action of **11a**. **11a** downregulates MyD88 expression and hence induces a partial uncoupling of TLR/IL-1R from NF-κB activation and consequent pro-inflammatory cytokine production that both initiates pathogenic IL-17-mediated inflammation and perpetuates chronic vascular permeability, inflammation, and pathology in the joints.[54,55] Thus **11a**-mediated downregulation of MyD88 impacting at one or more of these sites provides a molecular mechanism for the protection afforded in CIA.

responses. Although we have previously shown variation in inhibitory effects of small PC-containing molecules,[12] we did not observe any stimulatory effects. The reasons underlying such SMA-mediated promotion of TLR-driven cytokine responses, which potentially could reflect adjuvant-like applications for these compounds similar to those based on classical pro-inflammatory TLR ligands,[20] have not been investigated at this stage. However, the data underline the point that structurally closely related compounds may vary with respect to immunomodulatory activity and hence require careful analysis at the individual level.

On the basis of previous in vitro analysis of the effects of ES-62 on macrophages,[4,5] allied to its protective effects in CIA,[7−9] sulfone **11a** was selected from the in vitro screen as a molecule showing properties that might suggest activity against CIA similar to ES-62. We employed the dosing schedule used successfully with ES-62, which was based on the premise that exposing the mice to the parasite product both prior to and at the time of immunization will maximize the potential for modulating initiation of pathogenic immune responses while re-exposure at d21 in the antigen challenge phase will target ongoing and/or memory responses and therefore reflect a more therapeutic regime. This revealed that **11a** not only demonstrated efficacy against disease development that mirrored that of the parent molecule but in inhibiting IFNγ and to a lesser extent, IL-17 production, showed evidence of the same immunological mechanism of action. Our aim in this study was simply proof of concept that an SMA could afford protection using a regimen previously shown to be successful with ES-62, and thus it is possible that the molecule can be shown to be even more effective with optimization of dosage regimen. Further support for targeting of IL-17 responses is shown by **11a** mirroring ES-62 in preventing secretion by dendritic cells,

of cytokines involved in polarization and maintenance of Th17 cells, and inhibiting the subsequent ability of such DCs to prime Th17 responses. Moreover, **11a** is able to cause downregulation of the key signaling adaptor MyD88 in macrophages. This is consistent with its effects on NF-κB activation and explains its ability to mimic a primary mechanism of action of ES-62 in suppressing TLR-mediated cytokine production.[9,53] In addition, such targeting of MyD88 provides a molecular rationale (Figure 8D) for the protection against CIA afforded by **11a** as TLR/MyD88-dependent signaling has been proposed to be pathogenic in both CIA and RA. Moreover, the recent use of MyD88-deficient mice has shown this signaling element to be crucial to development of IL-17-driven arthritis, both in terms of initiation of pathogenic IL-17 responses and also the severity of joint inflammation and pathology.[17−20,54,55]

11a is of course too small to be immunogenic, but it also possesses another feature that increases its candidature as a more effective version of ES-62 for therapeutic purposes. It contains a tertiary dimethylamino group in contrast to the quaternary trimethylammonium choline component of PC; previously we have shown that unlike choline, its dimethylamino analogue does not compete for binding to the myeloma protein TEPC 15, an antibody which recognizes PC.[60] This suggests that **11a** will not bind to endogenous anti-PC antibodies that are found in humans and which could conceivably interfere with activity of PC-containing SMAs. Furthermore, there is increasing evidence that natural anti-PC antibodies by an as yet unknown mechanism may in themselves be anti-inflammatory, protecting humans from diseases such as atherosclerosis,[61] and so this represents another reason for designing drugs that avoid interacting with them. In this way, possessing the tertiary amine rather than quaternary

ammonium salt choline may result in a safer as well as a more effective drug.

Finally, although based on a combination of epidemiological evidence and model studies there has been much enthusiasm for the idea that parasitic worms may represent a starting point for novel drug design for diseases associated with aberrant inflammation, relevant studies are at an early stage and to date no actual drugs have been produced. However, the work presented in this paper serves as a strong proof of concept that novel small molecules can be active against severe and complex diseases in vivo. Moreover, the compounds described here benefit from ease of synthesis and active compounds such as **11a** can be readily subjected to further chemical manipulation to optimize properties as required. In general, this study suggests that there is great medicinal chemical potential to be found in synthetic libraries based around active moieties of helminth-derived molecules.

■ EXPERIMENTAL SECTION

Preparation of SMAs. For assay, all compounds tested were of greater than 95% purity. Compounds were reconstituted at 100 mg/mL in cell culture-tested DMSO (Sigma-Aldrich, UK), diluted in RPMI medium to 1 mg/mL, and stored in microcentrifuge tubes at −20 °C. Compounds were sterilized using a Millex-GP (0.22 μm) (Millipore, UK) filter unit prior to use in culture. All reagents and plastics used were sterile and pyrogen free.

General Methods for Synthesis. ^{1}H and ^{13}C NMR spectra were measured on a Bruker DPX-400 MHz spectrometer with chemical shifts given in ppm (δ values) relative to proton and carbon traces in solvent. Coupling constants are reported in Hz. IR spectra were recorded on a Perkin-Elmer 1 FT-IR spectrometer. Elemental analysis was carried out on a Perkin-Elmer 2400, analyzer series 2. Mass spectra were obtained on a Jeol JMS AX505. Anhydrous solvents were obtained from a Puresolv purification system, from Innovative Technologies, or purchased as such from Aldrich. Melting points were recorded on a Reichert hot-stage microscope and are uncorrected. Chromatography was carried out using 200−400 mesh silica gels or using reverse-phase HPLC on a Waters system using a C18 Luna column.

Declaration of Purity. All final compounds were equal or more than 95% pure by HPLC and ^{1}H NMR.

Diethyl 4-Bromobenzylphosphonate[62] (3a). 1-Bromo-4-(bromomethyl)benzene (3.10 g, 12.5 mmol) was suspended in triethylphosphite (2.4 mL, 13.7 mmol, 1.1 equiv), and the mixture was heated under reflux under N_2 for 6 h. Excess triethylphosphite was removed under reduced pressure to give the required product as a yellow oil (3.50 g, 91%). ^{1}H NMR (DMSO-d_6): δ 7.51 (2H, dd, J = 8.4 Hz and J = 0.9 Hz), 7.25 (2H, dd, J = 8.4 and 2.5 Hz), 3.96−3.91 (4H, m), 3.25 (2H, d, J = 21.6 Hz), 1.19 (6H, t, J = 7.1 Hz). ^{13}C NMR (DMSO-d_6): δ 131.9, 131.8, 131.0, 119.7, 61.4, 32.2, 16.2. IR (NaCl): 3447, 2982, 2462, 1646, 1513, 1488, 1392, 1249, 1093, 1057, 963, 853, 766 cm^{−1}. HRESIMS: calcd for $C_{11}H_{16}O_3{}^{79}BrP$, 306.0020; found, 306.0020.

Diethyl 4-Methylbenzylphosphonate[62] (3b). 1-(Bromomethyl)-4-methylbenzene (2.60 g, 14.0 mmol) was suspended in triethylphosphite (2.9 mL, 16.7 mmol), and the mixture was heated under reflux under N_2 for 20 h. Excess triethylphosphite was removed under reduced pressure to give the required product as a colorless oil (3.20 g, 94%). ^{1}H NMR (DMSO-d_6): δ 7.17 (2H, d, J = 8.4 Hz), 7.12 (2H, d, J = 8.4 Hz), 3.96−3.88 (4H, m), 3.17 (2H, d, J = 20 Hz), 2.27 (3H, s), 1.18 (6H, t, J = 7.1 Hz). ^{13}C NMR (DMSO-d_6): δ 135.4, 129.5, 129.1, 128.9, 61.2, 32.4, 20.6, 16.1. IR (NaCl): 3439, 2982, 2901, 2902, 1651, 1516, 1443, 1391, 1251, 1163, 1058, 963, 841, 783 cm^{−1}. HRESIMS: calcd for $C_{12}H_{19}O_3P$, 242.1072; found, 242.1069.

Diethyl 4-Nitrobenzylphosphonate[63] (3c). 1-(Bromomethyl)-4-nitrobenzene (2.44 g, 11.3 mmol) was suspended in triethylphosphite (5.0 mL, 28.79 mmol), and the mixture was heated under reflux under N_2 for 20 h. Excess triethylphosphite was removed under

reduced pressure to give the required product as a brown oil (6.60 g, 89%). ^{1}H NMR (DMSO-d_6): δ 8.19 (2H, d, J = 8.7 Hz), 7.58 (2H, dd, J = 8.7 Hz and J = 2.3 Hz), 4.07 (4H, q, J = 7.1 Hz), 3.48 (2H, d, J = 22.4 Hz), 1.19 (6H, t, J = 7.1 Hz). ^{13}C NMR (DMSO-d_6): δ 146.2, 141.0, 130.9, 123.2, 62.6, 32.9, 16.2. IR (NaCl): 3466, 2983, 1600, 1520, 1347, 1248, 1027, 966, 860, 796, 694 cm^{−1}. HRESIMS: calcd for $C_{11}H_{16}NO_5P$, 273.0766; found, 273.0763.

4-Bromobenzylphosphonic Acid[64] (4a). Diethyl 4-bromobenzylphosphonate (3.74 g, 12.20 mmol) was suspended in 12 M HCl (30 mL), and the mixture was heated under reflux for 48 h. The reaction mixture was concentrated under reduced pressure to give the required product as an off-white solid (2.20 g, 72%), mp 167−175 °C [slow decomposition]. ^{1}H NMR (DMSO-d_6): δ 9.71 (2H, br, s, OH), 7.47 (2H, d, J = 8.5 Hz), 7.20 (2H, d, J = 8.5 Hz), 2.97 (2H, d, J = 20.0 Hz). ^{13}C NMR (DMSO-d_6): δ 35.4, 34.1, 119.1, 130.8, 131.9, 133.8. IR (KBr): 2670, 2258, 1911, 1557, 1491, 1409, 1260, 1240, 1105, 999, 823, 703 cm^{−1}. HRESIMS: calcd for $C_7H_8{}^{79,81}BrO_3P$, 249.9394/251.9375; found, 249.9389/251.9375.

4-Methylbenzylphosphonic Acid[65] (4b). Diethyl 4-methylbenzylphosphonate (3.48 g, 14.40 mmol) was suspended in 12 M HCl (30 mL), and the mixture was heated under reflux for 56 h. The reaction mixture was concentrated under reduced pressure to give the required product as a white solid (1.99 g, 74%), mp 186−187 °C. ^{1}H NMR (DMSO-d_6): δ 9.58 (2H, br, s, OH), 7.14 (2H, d, J = 8.5 Hz), 7.08 (2H, d, J = 8.5 Hz), 2.92 (2H, d, J = 21.2 Hz), 2.26 (3H, s). ^{13}C NMR (DMSO-d_6): δ 135.2, 131.5, 129.95−129.94, 35.9, 21.4. IR (KBr): 2921, 2324, 1514, 1455, 1269, 1235, 1196, 1107, 996, 969, 946, 814, 740 cm^{−1}. HRESIMS: calcd for $C_8H_{11}O_3P$, 186.0445; found, 186.0446.

4-Nitrobenzylphosphonic Acid[66] (4c). Diethyl 4-nitrobenzylphosphonate (2.91 g, 10.60 mmol) was suspended in 12 M HCl (90 mL), and the mixture was heated under reflux for 18 h. The reaction mixture was concentrated under reduced pressure to give the required product as a brown solid (1.82 g, 93%), mp 208−214 °C [lit. mp 228−229 °C]. ^{1}H NMR (DMSO-d_6): δ 9.45 (2H, br, s, 2H, OH), 7.2−8.2 (4H, m), 2.98 (2H, d, J = 20.0 Hz).

2-{[(4-Bromobenzyl)(hydroxy)phosphoryl]oxy}-N,N,N-trimethylethanaminium Iodide (5a). 4-Bromobenzylphosphonic acid (0.700 g, 2.80 mmol) was suspended in thionyl chloride (5 mL), and the mixture was heated under reflux for 30 h under nitrogen. When the reaction mixture cooledd to room temperature, excess thionyl chloride was removed under reduced pressure and the residue was dissolved in chloroform (20 mL, dry). This solution was then transferred via syringe to a flame-dried, three-necked round-bottomed flask under nitrogen. This solution was then cooled to 0 °C, followed by the addition of pyridine (2 mL, dry) and the portionwise addition of choline iodide (0.82 g, 3.55 mmol). Stirring was continued for a further 3 days. The reaction mixture was concentrated under reduced pressure, and the residue was suspended in acetonitrile (2 mL). HPLC purification gave the required product as a colorless oil (0.071 g, 56%). ^{1}H NMR (DMSO-d_6): δ 7.47 (2H, d, J = 7.5 Hz), 7.24 (2H, d, J = 7.5 Hz), 4.18 (2H, br, s), 3.54 (2H, m), 3.04 (9H, s), 2.99 (2H, d, J = 20 Hz). ^{13}C NMR (DMSO-d_6): δ 139.7, 137.5, 136.4, 124.7, 70.9, 63.6, 58.7, 39.7, 38.4. IR (NaCl): 3383, 3030, 2957, 2913, 1896, 1767, 1686, 1485, 1337, 1241, 1202, 1163, 1093, 1012, 970, 830, 713 cm^{−1}. HRESIMS: calcd for $C_{12}H_{20}NO_3P^{79,81}Br$, 336.0364/338.0345; found, 336.0362/338.0339.

2-(Dimethylamino)ethyl Hydrogen 4-Bromobenzylphosphonate Trifluoroacetate (5b). 4-Bromobenzylphosphonic acid (0.455 g, 1.81 mmol) was suspended in thionyl chloride (5 mL), and the mixture was heated under reflux for 20 h. When the reaction mixture cooled to room temperature, excess thionyl chloride was removed under reduced pressure and the residue was dissolved in DCM (10 mL, dry). To this solution was added, at 0 °C, pyridine (400 μL, 4.9 mmol, dry) and dimethylethanolamine (122 μL, 2.2 mmol). The reaction mixture was stirred at room temperature for 5 h before the addition of water (1 mL). Stirring was continued for a further 20 h, after which time the solvent was removed under reduced pressure until ∼1 mL of crude solution was left. The crude mixture was then purified by reverse phase HPLC to give the required product as a colorless oil (295 mg, 37%) as a TFA salt. ^{1}H NMR (DMSO-d_6): δ 7.50 (2H, d, J =

7.8 Hz), 7.26 (2H, dd, J = 2.3 Hz and J = 8.4 Hz), 4.15−4.10 (2H, m), 3.29 (2H, t), 3.15 (2H, d, J = 21.4 Hz), 3.76 (6H, s). ^{13}C NMR (DMSO-d_6): δ 133.1, 131.8, 128.8, 119.4, 58.7, 56.7, 42.6, 32.1, 31.6. IR (NaCl): 3419, 3038, 2912, 2714, 2521, 1772, 1678, 1572, 1488, 1407, 1242, 1204, 1052, 1020, 836, 795, 720 cm^{-1}. HRESIMS: calcd for $C_{12}H_{20}NO_3P^{79,81}Br$, 336.0364/338.0345; found, 336.0362/338.0339.

2-(Dimethylamino)ethyl Hydrogen 4-Methylbenzylphosphonate Trifluoroacetate (5c). 4-Methylbenzylphosphonic acid (0.39 g, 2.10 mmol) was suspended in thionyl chloride (5 mL), and the mixture was heated under reflux for 20 h. When the reaction mixture cold to room temperature, excess thionyl chloride was removed under reduced pressure and the residue was dissolved in chloroform (20 mL, dry). To this solution was added, at 0 °C, pyridine (600 μL, 7.3 mmol, dry) and dimethylethanolamine (300 μL, 2.98 mmol). The reaction mixture was stirred at room temperature for 5 h before the addition of water (1 mL). Stirring was continued for a further 20 h, after which time the solvent was removed under reduced pressure until around 2 mL of crude solution was left. The crude mixture was then purified by reverse phase HPLC to give the required product as colorless oil (295 mg, 37%) as a TFA salt. ^{1}H NMR (DMSO-d_6): δ 7.17 (2H, dd, J = 2.1 Hz and J = 8.0 Hz), 7.10 (2H, d, J = 2.1 Hz), 4.09−4.05 (2H, m), 3.24 (2H, t), 3.05 (2H, d, J = 21.2 Hz), 2.72 (6H, s), 2.26 (3H, s). ^{13}C NMR (DMSO-d_6): δ 135.0, 130.6, 129.5, 128.6, 58.7, 56.9, 42.5, 33.7, 32.3, 20.6. IR (NaCl): 3418, 3030, 2964, 2921, 2714, 2528, 1766, 1682, 1515, 1472, 1416, 1321, 1203, 1088, 1020, 993, 832, 799, 720 cm^{-1}. HRESIMS: calcd for $C_{12}H_{21}O_3NP$, 258.1259; found, 258.1258.

2-(Dimethylamino)ethyl Hydrogen 4-Nitrobenzylphosphonate Trifluoroacetate (5d). 4-Nitrobenzylphosphonic acid (0.345 g, 1.59 mmol) was suspended in thionyl chloride (5 mL), and the mixture was heated under reflux for 20 h. When the reaction mixture cold to room temperature, excess thionyl chloride was removed under reduced pressure and the residue was dissolved in DCM (10 mL, dry). Pyridine (350 μL, 4.3 mmol, dry) and dimethylethanolamine (192 μL, 1.91 mmol) were added to the reaction mixture at 0 °C. The reaction mixture was stirred at room temperature for 5 h before the addition of water (1 mL). Stirring was continued for a further 20 h, after which time the solvent was removed under reduced pressure until ∼1 mL crude solution was left. The crude mixture was then purified by reverse phase HPLC to give the required product as colorless oil (200 mg, 31%) as a TFA salt. ^{1}H NMR (DMSO-d_6): δ 8.18 (2H, d, J = 8.2 Hz), 7.56 (2H, dd, J = 2.3 Hz and J = 8.8 Hz), 4.14−4.09 (2H, m), 3.31 (2H, d, J = 21.2 Hz), 3.25−3.23 (2H, m), 2.75 (6H, s). ^{13}C NMR (DMSO-d_6): δ 146.0, 142.7, 130.9, 123.1, 58.7, 56.9, 42.5, 34.3, 33.8. IR (KBr): 1767, 1680, 1514, 1472, 1414, 1320, 1202, 1087, 1020, 992, 832, 800, 721 cm^{-1}. HRESIMS: calcd for $C_{11}H_{18}O_5N_2P$, 289.0953; found, 289.0957.

3-(Dimethylamino)propyl Hydrogen 4-Methylbenzylphosphonate Trifluoroacetate (5e). 4-Methylbenzylphosphonic acid (0.25 g, 1.34 mmol), was suspended in thionyl chloride (7 mL), and the mixture was heated to reflux for 20 h. When the reaction mixture cold to room temperature, excess thionyl chloride was removed under reduced pressure and the residue was dissolved in chloroform (20 mL, dry). To this solution was added, at 0 °C, pyridine (295 μL, 3.6 mmol, dry) and 3-(dimethylamino)-1-propanol (190 μL, 1.60 mmol). The reaction mixture was stirred at room temperature for 5 h before the addition of water (1 mL). Stirring was continued for a further 20 h, after which time the solvent was removed under reduced pressure until around 2 mL of crude solution were left. The crude mixture was then purified by reverse phase HPLC to give the required product as a colorless oil (0.191 g, 37%) as a TFA salt. ^{1}H NMR (DMSO-d_6): δ 7.16 (2H, dd, J = 8.0 Hz and 2.0 Hz), 7.10 (2H, d, J = 8.0 Hz), 3.90 (2H, m), 3.03 (2H, d, J = 21.2 Hz), 3.01−2.98 (2H, m), 2.71 (6H, s), 2.27 (3H, s), 1.90−1.84 (2H, m). ^{13}C NMR (DMSO-d_6): δ 135.1, 130.5, 129.6, 128.6, 61.2, 53.8, 42.1, 33.8, 32.5, 25.1, 20.6. IR (NaCl): 3419, 3021, 2961, 2906, 2719, 2637, 1682, 1515, 1470, 1410, 1202, 1133, 1049, 971, 830, 719 cm^{-1}. HRESIMS: calcd for $C_{13}H_{23}NO_3P$, 272.1416; found, 272.1418.

tert-Butyl 4-Hydroxyphenylcarbamate[67] (6a). 4-Aminophenol (0.67 g, 6.14 mmol) was dissolved in DMF (15 mL, dry) under

nitrogen and the mixture cooled to 0 °C before the addition of BOC anhydride (1.40 g, 6.45 mmol). The mixture was gradually allowed to warm to room temperature, and stirring was continued for 20 h at room temperature. Solvent was removed under reduced pressure and the residue was dried in a drying pistol 60 °C for 2 h, to give the required product as an off-white solid (1.19 g, 93%), mp 146−148 °C [lit. mp 146 °C]. ^{1}H NMR (DMSO-d_6): δ 8.99 (1H, s, NH), 8.94 (1H, br, s, OH), 7.21 (2H, d, J = 8.6 Hz), 6.64 (2H, d, J = 8.6 Hz), 1.40 (9H, s). ^{13}C NMR (DMSO-d_6): δ 152.9, 152.5, 130.9, 120.0, 114.9, 78.4, 28.2. IR (KBr): 3361, 2975, 2936, 2876, 1696, 1610, 1531, 1436, 1370, 1231, 1165, 1058, 1029, 1014, 829, 803 cm^{-1}. HRESIMS: calcd for $C_{11}H_{15}NNaO_3$, 232.0950; found, (M + Na): 232.0951.

tert-Butyl 4-{[[3-(Dimethylamino)propoxy](hydroxy)phosphoryl]oxy} Phenylcarbamate Trifluoroacetate (6b). _tert_-Butyl 4-hydroxyphenylcarbamate (0.42 g, 2.00 mmol) was dissolved in chloroform (30 mL, dry) to which potassium carbonate (0.31 g, 2.20 mmol) and phosphorus oxychloride (0. 240 mL, 2.57 mmol) were added at 0 °C, under nitrogen. After 2 h, pyridine (2 mL, dry) and dimethylaminopropanol 0.30 mL, 2.54 mmol) were added. The mixture was stirred at 0 °C for 30 min then allowed to warm to room temperature. Stirring was continued for 72 h. Solvent was removed under reduced pressure, and the residue by HPLC purification gave the required product as white solid (0.012 g, 16%), mp 144−146 °C. ^{1}H NMR (DMSO-d_6): δ 9.25 (1H, br, s, NH), 7.38 (2H, d, J = 8.6 Hz), 7.06 (2H, d, J = 8.6 Hz), 1.90 (2H, t), 1.46 (9H, s). ^{13}C NMR (DMSO-d_6): δ 153.7, 147.3, 136.4, 121.1, 120.0, 79.8, 62.7, 54.9, 42.7, 29.0, 26.7. IR (KBr): 3414, 2981, 2929, 1700, 1605, 1513, 1410, 1393, 1311, 1214, 1161, 1054, 967, 841, 773, 701 cm^{-1}. HRESIMS: calcd for $C_{16}H_{27}N_2O_6P$, 375.1685; found, 375.1684.

2-[(4-Bromobenzyl)sulfanyl]ethanol (7a). 1-Bromo-4-(bromomethyl)benzene (10.00 g, 40.00 mmol), 2-mercaptoethanol (3.13 g, 40.00 mmol), and K_2CO_3 (5.53 g, 40.00 mmol, anhydrous) were added to DCM (50 mL, dry) at room temperature with stirring. Stirring was continued for 48 h, after which time water was added and then the reaction mixture was extracted with DCM. The organic layer was collected, dried (MgSO$_4$), filtered, and the solvent removed under reduced pressure to give the required product as a pale-yellow oil (11.00 g, 99%). ^{1}H NMR (CDCl$_3$): δ 7.46 (2H, d, J = 8.0 Hz), 7.22 (2H, d, J = 8.0 Hz), 3.71 (2H, s), 3.70 (2H, t, J = Hz), 2.65 (2H, t, J = 8.0 Hz), 1.93 (1H, br, s, OH). ^{13}C NMR (CDCl$_3$): δ 137.4, 131.9, 130.8, 121.3, 60.6, 35.4, 34.6. IR (thin film): 3390 (br), 2919, 1901, 1663, 1589, 1486, 1402, 1289, 1198, 1096, 1069, 1011, 881, 821 cm^{-1}. HRESIMS: calcd for $C_9H_{11}^{79,81}BrOS$, 245.9714/247.9693; found, 245.9712/245.9692.

2-[(4-Methylbenzyl)sulfanyl]ethanol[68] (7b). 1-(Bromomethyl)-4-methylbenzene (10.00 g, 54.03 mmol), 2-mercaptoethanol (4.22 g, 54.03 mmol), and K_2CO_3 (7.47 g, 54.03 mmol, anhydrous) were added to DCM (50 mL, dry) at room temperature with stirring. The stirring was continued for 48 h. Water was added, and the reaction mixture was extracted with DCM. The organic layer was collected, dried (MgSO$_4$), filtered, and the solvent removed under reduced pressure to give the required product as a pale-yellow oil (9.60 g, 98%). ^{1}H NMR (DMSO-d_6): δ 7.23 (2H, d, J = 8.0 Hz), 7.14 (2H, d, J = 8.0 Hz), 4.79 (1H, t, J = 14.3 Hz, OH), 3.72 (2H,s), 3.57 (2H, m), 2.52 (2H, t, J = 14.3 Hz), 2.30 (3H, s). ^{13}C NMR (DMSO-d_6): δ 135.7, 135.6, 128.8, 128.7, 60.6, 35.0, 33.3, 20.6. IR (KBr): 1664, 1513, 1422, 1386, 1098, 1068, 1020, 878, 817, 726 cm^{-1}. HRESIMS: calcd for $C_{10}H_{14}OS$, 182.07654; found, 182.0764.

2-[(4-Bromobenzyl)sulfonyl]ethanol (8a). 2-[(4-Bromobenzyl)sulfonyl]ethanol (11.00 g, 44.7 mmol) was dissolved in DCM (50 mL, dry) to which _m_-CPBA (21.10 g, 122.3 mmol) was added at room temperature with stirring. The reaction was slightly exothermic. The reaction mixture was stirred at room temperature overnight. Then 15 min after the addition of _m_-CPBA, a white solid material precipitated. NaHCO$_3$ (saturated) was added, and the reaction mixture was extracted. The organic layer was extracted with brine and collected, dried (MgSO$_4$), filtered, and the solvent removed under reduced pressure. The crude product was applied to a gel column chromatography using ethyl acetate/_n_-hexane 1/1, R_F = 0.1 to give the pure material as white crystals (4.47 g, 36%) after recrystallization

from ethyl acetate/*n*-hexane, mp 97−99 °C. ¹H NMR (DMSO-*d₆*): δ 7.61 (2H, d, *J* = 8.0 Hz), 7.37 (2H, d, *J* = 8.0 Hz), 5.21 (1H, br s, OH), 4.48 (2H, s), 3.83 (2H, t, *J* = 14.3 Hz), 3.18 (2H, t, *J* = 14.3 Hz). ¹³C NMR (DMSO-*d₆*): δ 133.2, 131.3, 128.1, 121.8, 58.8, 54.9, 53.9. IR (KBr): 3480 (br), 2991, 2928, 1490, 1408, 1388, 1291, 1262, 1235, 1115 (s), 1064, 1014, 848, 808, 705, 523 cm⁻¹. HRESIMS: calcd for $C_9H_{11}{}^{79/81}BrO_3S$, 277.9612/279.9592; found, 277.9614/279.9586.

2-[(4-Methylbenzyl)sulfonyl]ethanol (8b). 2-[(4-Methylbenzyl)sulfanyl]ethanol (9.60 g, 52.7 mmol) was dissolved in DCM (50 mL, dry) to which *m*-CPBA (18.18 g, 105.0 mmol, 2.0 mol equiv) was added at room temperature with stirring. The reaction was slightly exothermic. The reaction mixture was stirred at room temperature overnight. Then 15 min after the addition of *m*-CPBA, a white solid material precipitated. NaHCO₃ (saturated) was added, and the reaction mixture was extracted. The organic layer was extracted with brine and collected, dried (MgSO₄), filtered, and the solvent removed under reduced pressure. The crude product was recrystallized from ethyl acetate/*n*-hexane to give the pure material as white crystals (3.11 g). The mother liquor was applied to a silica gel column chromatography using ethyl acetate/*n*-hexane 1/1 (*R*_F = 0.2 and *R*_F = 0.5) to give an additional amount (0.40 g). The total amount obtained was (3.51 g, 31%), mp 102−104 °C. ¹H NMR (DMSO-*d₆*): δ 7.30−7.28 (2H, d, *J* = 8.0 Hz), 7.21−7.19 (2H, d, *J* = 8.0 Hz), 5.29 (1H, br, s, OH), 4.41 (2H, s), 3.82−3.79 (2H, t, *J* = 14.3 Hz), 3.14−3.11 (2H, t, *J* = 14.3 Hz), 2.31 (3H, s). ¹³C NMR (DMSO-*d₆*): δ 137.6, 130.9, 128.9, 125.6, 59.3, 54.9, 53.7, 20.7. IR (KBr): 1697, 1517, 1419, 1296 (s), 1263, 1175, 1116 (s), 1063, 1012, 848, 549, 489 cm⁻¹. HRESIMS: calcd for $C_{10}H_{14}O_3S$, 214.0664; found, 214.0665.

1-Bromo-4-[(vinylsulfonyl)methyl]benzene (9a). 2-[(4-Bromobenzyl)sulfonyl]ethanol (2.00 g, 7.17 mmol) was dissolved in DCM (25 mL, dry) to which triethylamine (3 mL, 2.18 g, 21.52 mmol, 3.0 mol equiv, anhydrous) was added followed by methylsulfonyl chloride (2 mL, 3.12 g, 19.14 mmol, 2.7 mol equiv) at 0 °C with stirring, which was continued at room temperature overnight. The reaction mixture was basified with sodium hydrogen carbonate (saturated). The organic layer was collected after the extraction, dried over (MgSO₄), filtered, and the solvent removed under reduced pressure. The crude product was applied to a silica gel column chromatography using ethyl acetate/*n*-hexane (1/2, *R*_F = 0.4). The required product (1.60 g, 86%) was obtained as a white solid, mp 95−97 °C. ¹H NMR (DMSO-*d₆*): δ 7.60 (2H, d, *J* = 8.4 Hz), 7.32 (2H, d, *J* = 8.4 Hz), 6.96 (1H, dd, *J* = 16.8 Hz and *J* = 9.9 Hz), 6.21 (1H, d, *J* = 8.0 Hz), 6.09 (1H, d, *J* = 16.6 Hz), 4.55 (2H, s). ¹³C NMR (DMSO-*d₆*): δ 136.2, 133.1, 131.3, 130.5, 128.1, 121.9, 58.0. IR (KBr): 3437, 3057, 2981, 2932, 1489, 1408, 1309, 1260, 1161, 1121, 1072, 1014, 976, 843, 795, 714,519 cm⁻¹. HRESIMS: calcd for $C_9H_9{}^{79/81}BrO_2S$, 259.9507/261.9486; found, 259.9506/261.9484.

2-[(4-Methylbenzyl)sulfonyl]ethyl Methanesulfonate and 1-Methyl-4-[(vinylsulfonyl)methyl]benzene (9b) and (10b). 2-[(4-Methylbenzyl)sulfonyl]ethanol (3.110 g, 14.51 mmol) was dissolved in DCM (25 mL, dry) to which triethylamine (2.202 g, 21.77 mmol, 1.5 mol equiv, anhydrous) was added, followed by methylsulfonyl chloride (2.493 g, 21.77 mmol, 1.5 mol equiv) at 0 °C with stirring, which was continued at room temperature overnight. The reaction mixture was basified with sodium hydrogen carbonate (saturated). The organic layer was collected after the extraction, dried (MgSO₄), filtered, and the solvent removed under reduced pressure. The crude product was obtained as a yellow semisolid (5.060 g). TLC showed two spots: *R*_F = 0.3 and *R*_F = 0.6 (ethyl acetate/*n*-hexane 1/1). This mixture was used in the next step without further purification.

N-{2-[(4-Bromobenzyl)sulfonyl]ethyl}-N,N-dimethylamine (11a). 1-Bromo-4-[(vinylsulfonyl)methyl]benzene (1.600 g, 6.12 mmol) was dissolved in DCM (25 mL, dry) to which dimethylamine (4 mL, 2 M in THF) was added at room temperature with stirring. The stirring was continued at room temperature overnight. The reaction mixture was extracted with a saturated solution of sodium carbonate. The organic layer was collected, dried over (MgSO₄), and filtered, and the solvents were removed under reduced pressure, after which the crude product was applied to a silica gel column chromatography using ethyl acetate/*n*-hexane (1/1) in the first

instance, followed by ethyl acetate/methanol (9/2, *R*_F = 0.5). The product was obtained as a white solid material (1.36 g, 73%) after trituration with *n*-hexane, mp 58−60 °C. ¹H NMR (DMSO-*d₆*): δ 7.64 (2H, d, *J* = 8.0 Hz), 7.37 (2H, d, *J* = 8.0 Hz), 4.52 (2H, s), 3.22 (2H, t, *J* = 14.3 Hz), 2.67 (2H, t, *J* = 14.3 Hz), 2.17 (6H, s). ¹³C NMR (DMSO-*d₆*): δ 133.1, 131.4, 127.9, 121.9, 57.9, 51.6, 49.4, 44.7. IR (KBr): 3424, 2979, 2942, 2822, 2772, 1591, 1488, 1408, 1295, 1275, 1118, 1051, 1013, 843, 816, 640,513 cm⁻¹. HRESIMS: calcd for $C_{11}H_{16}{}^{79/81}BrNO_2S$, 305.0085/307.0065; found, 305.0081/307.0066.

N,N-Dimethyl-2-[(4-methylbenzyl)sulfonyl]ethanamine (11b). The product from the previous experiment (4.880 g) was dissolved in DCM (50 mL, dry) to which dimethylamine (4 mL, 2 M in THF) was added at room temperature with stirring. The stirring was continued at room temperature overnight, after which time the reaction mixture was extracted with a saturated solution of sodium carbonate. The organic layer was collected, dried (MgSO₄), and filtered, and the solvents were removed under reduced pressure and the crude product was applied to a silica gel column chromatography eluted with ethyl acetate/*n*-hexane (1/1, *R*_F = 0.1) in the first instance, followed by ethyl acetate/methanol (9/1). The product was obtained as white solid material (2.200 g, 63% based on 2-[(4-methylbenzyl)sulfonyl]ethanol) after trituration with *n*-hexane, mp 68−70 °C. ¹H NMR (DMSO-*d₆*): δ 7.28 (2H, d, *J* = 8.0 Hz), 7.21 (2H, d, *J* = 8.0 Hz), 4.44 (2H, s), 3.17 (2H, t, *J* = 14.3 Hz), 2.65 (2H, t, *J* = 14.3 Hz), 2.31 (3H, s), 2.16 (6H, s). ¹³C NMR (DMSO-*d₆*): δ 137.7, 130.8, 129.0, 125.4, 58.4, 51.6, 49.0, 44.9, 20.7. IR (KBr): 1511, 1463, 1399, 1380, 1314, 1258, 1156, 1119, 1050, 892, 853, 822, 749 cm⁻¹. HRESIMS: calcd for $C_{12}H_{19}NO_2S$, 241.1136; found, 241.1139.

N,N,N-Trimethyl-2-1(4-bromobenzyl)sulfonyl{ethanaminium methane sulfonate (12a). 2-[(4-Bromobenzy)lsulfonyl]ethyl methanesulfonate (0.06g, 0.17 mmol) was suspended in trimethylamine (5 mL in toluene), and the mixture was stirred at room temperature under nitrogen for a period of 5 d, then heated to 60 °C for 20 h. The solvent was concentrated under reduced pressure to give an off-white solid (0.045 g, 83%), mp 187−188 °C. ¹H NMR (DMSO-*d₆*): δ 7.66−7.64 (2H, d, *J* = 8.0 Hz), 7.40−7.38 (2H, d, *J* = 8.0 Hz), 4.64(2H, s), 3.85−3.80 (2H, m), 3.78−3.74 (2H, m), 3.12 (9H, s). ¹³C NMR (DMSO-*d₆*): δ 133.1, 131.6, 126.3, 121.9, 57.6, 57.4, 52.5, 44.2. IR (KBr): 1591, 1489, 1424, 1413, 1360, 1318, 1277, 1193, 1140, 1068, 1040, 1011, 790, 770 cm⁻¹. HRESIMS: calcd for $C_{12}H_{19}{}^{79/81}BrNO_2S$, 320.0320/322.0300; found, 320.0321/322.0297.

N,N,N-Trimethyl-2-[(4-methylbenzyl)sulfonyl]ethanaminium Iodide (12b). N,N-Dimethyl-2-[(4-methylbenzyl)sulfonyl]-ethanamine (0.950 g, 3.94 mmol) was dissolved in DCM (25 mL, dry) to which iodomethane (4 mL) was added with stirring at room temperature. The stirring was continued overnight. The white solid material formed was filtered off and dried under reduced pressure (1.490 g, 99%), mp 212−214 °C. ¹H NMR (DMSO-*d₆*): δ 7.33 (2H, d, *J* = 8.0 Hz), 7.25 (2H, d, *J* = 8.0 Hz), 4.58 (2H, s), 3.83−3.79 (2H, m), 3.74−3.71 (2H, m), 3.12 (9H, s), 2.33 (3H, s). ¹³C NMR (DMSO-*d₆*): δ 138.1, 131.0, 129.2, 124.3, 57.9, 57.3, 52.5, 45.0, 18.6. IR (KBr): 1514, 1486, 1326, 1257, 1153, 1123, 1015, 882 cm⁻¹. HRESIMS: calcd for $C_{13}H_{22}NO_2S$, 256.1371; found, 256.1375.

Similarly, the following were prepared: **11c−11p, 12c−12d, 16d−16f, 17d−17f.**

N¹,N¹,N²-Trimethyl-N²-[2-(phenylsulfonyl)ethyl]-1,2-ethane-diamine (18a). (Vinylsulfonyl)benzene (commercially available) (100 mg, 0.60 mmol) was dissolved in DCM (4 mL, dry) to which N¹,N¹,N²-trimethyl-1,2-ethanediamine (61 mg, 0.062 mL, 0.60 mmol) was added at room temperature with stirring. Stirring was continued at room temperature overnight. The solvent was removed under reduced pressure to give the required product as a clear pale-yellow oil in quantitative yield. ¹H NMR (DMSO-*d₆*): δ 7.93 (2H, t, *J* = 7.3 Hz), 7.77 (1H, t, *J* = 7.3 Hz), 7.68 (2H, t, *J* = 7.3 Hz), 3.49 (2H, t, *J* = 7.2 Hz), 2.68 (2H, t, *J* = 7.4 Hz), 2.31 (2H, t, *J* = 7.4 Hz), 2.13 (2H, t, *J* = 7.4 Hz), 2.05 (9H, s). IR: 1682, 1606, 1449, 1300, 1199, 1143, 1084, 1037, 744, 731, 689 cm⁻¹. LRESIMS: calcd for $C_{13}H_{23}N_2O_2S$, 271.40; found, 271.39.

Similarly, the following were prepared: **18b−18l.**

N-[2-(Dimethylamino)ethyl](phenyl)methanesulfonamide (19a). Phenylmethanesulfonyl chloride [commercially available] (1.034 g, 5.416 mmol) was dissolved in dichloromethane (10 mL, dry) to which N^1,N^1-dimethyl-1,2-ethanediamine [commercially available] (0.477 g, 5.416 mmol) dissolved in dichloromethane (20 mL, dry) was added dropwise at room temperature with stirring under nitrogen. The reaction mixture was stirred at room temperature for 4 days. The reaction mixture was washed with aqueous sodium hydroxide solution (318 mg, 7.95 mmol in 10 mL). The organic layer was separated, dried (MgSO₄), and the solvent removed under reduced pressure to give the required product as a white microcrystalline solid (1.100 g, 84%), mp 127−129 °C, R_F = 0.1 [TLC: basic, 99% ethyl acetate and 1% TEA]. ¹H NMR (DMSO-d_6): δ 7.38−7.32 (5H, m), 6.93 (1H, br), 4.35 (2H, s), 2.93 (2H, t, J = 6.7 Hz), 2.25 (2H, t, J = 6.9 Hz), 2.11 (6H, s). IR [KBr]: 1495, 1458, 1415, 1327, 1261, 1128, 1149, 1050, 893, 784 cm⁻¹. Calculated for $C_{11}H_{18}N_2O_2S$: C, 54.52; H, 7.49; N, 11.56; S, 13.23. Found: C, 54.76; H, 7.48; N, 11.62; S, 13.49. HRFABMS: calcd for $C_{11}H_{19}O_2N_2S$, 243.1167; found, 243.1169.

Similarly, the following were prepared: **19b−19z**.

N-[2-(4-Morpholinyl)ethyl](2-naphthyl)methanesulfonamide (19u). 2-Naphthylmethanesulfonyl chloride (50 mg, 0.208 mmol) was dissolved in dichloromethane (1 mL, dry) to which 2-(4-morpholinyl)ethanamine [commercially available] (27 mg, 34 μL, 0.208 mmol) was added neat dropwise at room temperature with stirring under nitrogen. The reaction mixture was stirred at room temperature overnight. The reaction mixture was washed with aqueous sodium hydroxide solution (123 mg, 3.08 mmol in 6 mL). The organic layer was separated, dried (MgSO₄), and the solvent removed under reduced pressure. The product was obtained as a white solid after recrystallization from ethyl acetate/n-hexane (60 mg, 86%), mp 131−134 °C, R_F = 0.2 [ethyl acetate only]. ¹H NMR (DMSO-d_6): δ 7.92−7.90 (4H, m), 7.54−7.51 (3H, m), 6.96 (1H, br), 4.55 (2H, s), 3.55 (4H, t, J = 4.8 Hz), 3.05 (2H, t, J = 6.8 Hz), 2.36−2.32 (6H, m). IR (KBr): 1676, 1642, 1594, 1561, 1506, 1462, 1423, 1308, 1174, 1118, 1070, 980, 911, 870, 823, 752, 722 cm⁻¹. Calculated for $C_{17}H_{22}N_2O_3S$: C, 61.05; H, 6.63; N, 8.38. Found: C, 61.12; H, 6.73; N, 8.01. HREIMS: calcd for $C_{17}H_{22}O_3N_2S$, 334.1351; found, 334.1352.

Similarly, the following were prepared: **19v−19w**.

N-Benzylethylenesulfonamide (20a). Benzylamine (1.275 g, 11.89 mmol) was dissolved in DCM (5 mL, dry) at 0 °C with stirring under N₂ to which a solution of 2-chloroethanesulfonyl chloride (0.969 g, 5.94 mmol) dissolved in DCM (5 mL, dry) was added at 0 °C with stirring under N₂, after which time the reaction mixture was stirred at room temperature for 2 h. The reaction mixture was extracted with dilute hydrochloric acid, and the organic layers were collected, dried (MgSO₄), filtered, and the solvent removed under reduced pressure. The crude product was purified by column chromatography (ethyl acetate/n-hexane 1/3, R_F = 0.2). The product was obtained as colorless oil (390 mg, 33%). ¹H NMR (DMSO-d_6): δ 7.82 (1H, t, J = 6.3 Hz), 7.35−7.25 (5H, m), 6.69 (1H, dd, J = 10.0 and 16.5 Hz), 6.04 (1H, d, J = 16.5 Hz), 5.95 (1H, d, J = 10.0 Hz), 4.04 (2H, d, J = 6.2 Hz). IR (NaCl): 1497, 1456, 1385, 1327, 1148, 1061, 971, 843, 740 cm⁻¹. Calculated for $C_9H_{11}NO_2S$: C, 54.80; H, 5.62; N, 7.10. Found: C, 54.89; H, 5.72; N, 7.04. HRCIMS: calcd for $C_9H_{12}O_2NS$, 198.0589; found, 198.0590.

N-Benzyl-2-(1-pyrrolidinyl)ethanesulfonamide: (21a). Benzylethylenesulfonamide (140 mg, 0.709 mmol) was dissolved in DCM (5 mL, dry) at room temperature to which pyrrolidine (500 mg; 590 μL, 7.09 mmol) was added at room temperature with stirring. The reaction mixture was left standing at room temperature for 48 h. Solvent and excess pyrrolidine were removed under reduced pressure. The white solid material obtained was triturated with n-hexane and filtered to give the required product as a white solid (135 mg, 71%), R_F = 0.2 (ethyl acetate/NMM 100/1; basic TLC), mp 100−103 °C. ¹H NMR (DMSO-d_6): δ 7.60 (1H, t, J = 6.2 Hz), 7.36−7.24 (5H, m), 4.15 (2H, d, J = 6.2 Hz), 3.11 (2H, t, J = 7.5 Hz), 2.71 (2H, t, J = 7.9 Hz), 2.37−2.32 (4H, m), 1.67−1.63 (4H, m). IR (KBr): 1642, 1458, 1331, 1133, 1072, 1017, 870, 761, 738, 705 cm⁻¹. Calculated for $C_{13}H_{20}N_2O_2S$: C,

58.18; H, 7.51; N, 10.44. Found: C, 58.03; H, 7.84; N, 10.32. HRFABMS: calcd for $C_{13}H_{21}O_2N_2S$, 269.1324; found, 269.1325.

Similarly, the following were prepared: **21b−21r**.

N-Phenylethylenesulfonamide (22). Aniline (1.59 g, 17.12 mmol) was dissolved in DCM (25 mL, dry) at 0 °C with stirring under N₂ to which NMM (1.73 g; 1.88 mL; 17.12 mmol) was added with stirring. 2-Chloroethanesulfonyl chloride (2.79 g, 1.80 μL, 17.12 mmol) was added at room temperature with stirring under N₂. The reaction mixture was stirred at room temperature for 2 h. The reaction mixture was then extracted with dilute hydrochloric acid, and the organic layers were collected, dried (MgSO₄), filtered, and the solvent removed under reduced pressure. The crude product was purified by column chromatography (ethyl acetate/n-hexane 1/3, R_F = 0.3). The product was obtained as a light-brown solid (1.918 g, 61%) after trituration with n-hexane, mp 54−57 °C [lit¹. mp 64−67 °C; lit.² mp 65 °C]. ¹H NMR (DMSO-d_6): δ 9.96 (1H, s), 7.31−7.26 (1H, 2, m), 7.15−7.12 (2H, m), 7.08 (1H, t, J = 7.3 Hz), 6.79 (1H, dd, J = 10.0 and 16.5 Hz), 6.11 (1H, d, J = 16.5 Hz), 6.03 (1H, d, J = 10.0 Hz). IR (KBr): 1597, 1488, 1410, 1321, 1218, 1151, 968, 924, 751 cm⁻¹. Calculated for $C_8H_9NO_2S$: C, 52.44; H, 4.95; N, 7.64. Found: C, 52.33; H, 4.85; N, 7.54. HREIMS: calcd for $C_8H_9NO_2S$, 183.0354; found, 183.0350.

2-(Dimethylamino)-N-phenylethanesulfonamide[69] (23a). N-Phenylethylenesulfonamide (300 mg, 1.64 mmol) was dissolved in dichloromethane (5 mL, dry) to which dimethylamine (2 mL, 2.0 M solution in THF) was added at room temperature with stirring. The reaction mixture was stirred at room temperature overnight. Volatile material was removed under reduced pressure, and the crude product obtained was applied to a silica gel column chromatography. The product was eluted with ethyl acetate/NMM (100/1), R_F = 0.3. The required product was obtained as a white solid after recrystallization from ethyl acetate/n-hexane (340 mg, 91%), mp 68−71 °C [lit. mp 64−65 °C]. ¹H NMR (DMSO-d_6): δ 9.77 (1H, br), 7.33−7.06 (5H, m), 3.19 (2H, t, J = 7.4 Hz), 2.62 (2H, t, J = 7.4 Hz), 2.05 (6H, s). Calculated for $C_{10}H_{16}N_2O_2S$: C, 52.61; H, 7.06; N, 12.27. Found: C, 52.75; H, 7.25; N, 12.14.

Similarly, the following were prepared: **23b−23h**.

N-[2-(Dimethylamino)ethyl]-2-phenylacetamide[70−72] (24a). N^1,N^1-Dimethyl-1,2-ethanediamine (500 mg, 620 μL, 5.67 mmol) was dissolved in DCM (15 mL, dry). Phenylacetyl chloride (877 mg, 5.67 mmol) was dissolved in DCM (15 mL, dry) then added dropwise with stirring at 0 °C to the amine solution. Stirring was continued overnight at room temperature. The reaction mixture was extracted with sodium hydroxide solution (500 mg in 25 mL of water). The organic layer was collected and dried (MgSO₄), and the solvent was removed under reduced pressure. The crude product was purified by column chromatography using ethyl acetate/NMM/methanol (98/1/1) to give the product as white crystals (0.940 g, 80%), mp 40−42 °C. ¹H NMR (DMSO-d_6): δ 7.92 (1H, br), 7.29−7.17 (5H, m), 3.38 (2H, s), 3.14 (2H, q, J = 6.8 Hz), 2.27 (2H, t, J = 6.8 Hz), 2.11 (6H, s). IR (KBr): 1652, 1554, 1459, 1354, 1314, 1268, 1188, 1086, 859, 701 cm⁻¹. Calculated for $C_{12}H_{18}N_2O$: C, 69.87; H, 8.80; N, 13.58. Found: C, 69.94; H, 8.84; N, 14.11. HRFABMS: calcd for $C_{12}H_{19}N_2O$, 207.1497; found, 207.1498.

Similarly, the following were prepared: **24b−24e, 25a−25d**.

Biological Studies. Mice. Mice were bred and/or maintained in accordance with the Home Office UK licenses PPL60/3580, PPL60/3119, and PIL60/12183 and the Ethics Review Board of the Universities of Glasgow and Strathclyde. Collagen-induced arthritis (CIA) was induced in male DBA/1 mice (8−10 weeks old; Harlan Olac; Bicester, UK) by intradermal immunization with bovine type II collagen (CII, MD Biosciences, Switzerland) in complete Freund's adjuvant (CFA) on day 0 and by intraperitoneal challenge (in PBS) on day 21. Mice were treated with purified endotoxin-free PC-BSA, BSA (both 2 μg/dose; prepared as previously described[8]), and the absence of endotoxin confirmed using an Endosafe kit (Charles River Laboratories, UK), **11a** (1 μg/dose), or PBS subcutaneously on days −2, 0, and 21 and arthritis scored as previously described.[7−9]

Ex Vivo Analysis. Isolated draining lymph node (DLN) cells (10⁶/mL) were stimulated in RPMI medium supplemented with 10% heat-

inactivated fetal calf serum (HI FCS), 2 mM L-glutamine, 50 U/mL penicillin, and 50 μg/mL streptomycin (all from Gibco Life Technologies, UK) (complete RPMI) $\pm$ 50 ng/mL phorbol 12-myristate 13-acetate (PMA; Sigma-Aldrich, UK) plus 500 ng/mL ionomycin (Sigma-Aldrich) before addition of 10 μg/mL Brefeldin A (Sigma-Aldrich) for 5 h at 37 °C with 5% CO_2. Phenotypic markers were labeled using anti-CD4-PERCP, anti-CD8-FITC, or anti-$\gamma\delta$-PE (BioLegend, UK) antibodies before the cells were fixed and permeabilized using BioLegend protocols. Cells were then labeled using anti-IFNγ-Pacific Blue and anti-IL-17A-APC (BioLegend) antibodies for 30 min prior to flow cytometry and gated according to appropriate isotype controls.[9] IL-17 levels were measured in serum as described previously.[9]

Cell Biology Studies. *Generation of Bone Marrow-Derived Macrophages (bmMs).* Bone marrow was isolated from mouse femurs from 6−8 week-old, male BALB/c mice and cells cultured for 7 days at 37°/5% CO_2 in complete Dulbecco's Modified Eagle's Medium (DMEM; Gibco Life Technologies) supplemented with 20% L929 cell culture supernatant (contains CSF-1), 20% HI FCS, 2 mM L-glutamine, 50 U/mL penicillin, and 50 μg/mL streptomycin with fresh medium being added on day 4.[5] The cells were analyzed by flow cytometry and were shown routinely to be $\geq$99% positive for CD11b (BD Pharmingen, UK) and F4/80 markers (eBioscience, UK).

Cell Culture and Cytokine Analysis by Enzyme-Linked Immunosorbent Assay (ELISA). BmMs were cultured in RPMI complete medium in triplicate (2×10^5 cells/well) in 96-well plates and were rested overnight prior to stimulation with 5 μg/mL of the relevant compounds diluted in complete RPMI for 18 h. In some experiments, bmMs were then stimulated with either 100 ng/mL *Salmonella Minnesota* LPS (Sigma-Aldrich, UK), 10 ng/mL BLP (Pam3CSK4; Axxora Ltd., UK), or 0.01 μM CpG (Source Bioscience Autogen, UK) for 24 h. Culture supernatants were then removed and stored at −20 °C until analysis. ELISAs for IL-12p40 and IL-6 cytokines (limit of sensitivity: 16 pg/mL) were performed using paired antibodies from BD Bioscience Pharmingen.

TransAM (NFκB p65). BmMs were cultured in 6-well plates (4×10^6 cells/well) in complete RPMI medium. After 24 h, the medium was changed and the cells were pretreated with the compounds (5 μg/mL) for 18 h before being stimulated with 100 ng/mL LPS, 10 ng/mL BLP, or 1 μM CpG for 1 h. The ability of the compounds per se to activate NFκB p65 was also tested. Activated NFκB p65 was measured in nuclear fractions (isolated using a Nuclear Extraction Kit; ActiveMotif, UK) by the ELISA-based TransAM kit (ActiveMotif) according to the manufacturer's instructions.

Flow Cytometric Analysis of bmMs. Cell viability was determined by 7-amino actinomycin D (7-AAD; BD Pharmingen) staining. BmMs (2×10^5/well) were pretreated with **11a** (5 μg/mL) or ES-62 (2 μg/mL) for 18 h prior to being stimulated with either 100 ng/mL LPS, 10 ng/mL BLP, or 0.01 μM CpG for 24 h. The ability of the compounds alone to induce cell death was also tested. The cells were washed in PBS containing 1% FCS, then subsequently incubated with 5 μL of 7-AAD for 10 min on ice in the dark. Flow cytometry was conducted using a FACSCanto system (Becton Dickinson Pharmingen) and the data processed by FlowJo software (Tree Star Inc., USA).

Flow cytometric analysis of MyD88 expression was performed using a rabbit anti-mouse MyD88 antibody (ab2068; Abcam) and FITC-conjugated goat anti-rabbit IgG (Vector Laboratories). Prior to staining, dead cells were discriminated by use of LIVE/DEAD stain (Aqua; Invitrogen) before being fixed and permeabilized using BioLegend reagents and protocols. Flow cytometry was conducted using the LSRII system (Becton Dickinson Pharmingen) and the data processed by FlowJo software (Tree Star Inc., USA).

Measurement of Dendritic Cell-Derived Cytokines and Th17 Polarization. Bone marrow-derived dendritic cells (bmDCs) from femurs of C57BL/6 or BALB/c mice (6−8 weeks old) were derived by in vitro culture in complete RPMI 1640 medium (containing 2 mM glutamine, 50 U/mL penicillin, 50 μg/mL streptomycin, and 10% FCS) supplemented with recombinant murine GM-CSF (10 ng/mL, Peprotech Inc.). Naïve CD4+CD62L+ T cells were isolated from lymph nodes using magnetic bead technology according to the manufacturer's instructions (Miltenyi). For bmDC-T cell cocultures, bmDCs were incubated $\pm$ **11a** (5 μg/mL) prior to treatment $\pm$ LPS from *S. minnesota* and then pulsed with ovalbumin (OVA) peptide (0−300 nM) before incubation with naïve T cells derived from OVA-specific DO.11.10/BALB/c or OT-II/C57BL/6 mice for 3 d. Conditioned medium from DC cultures and DC-T cell cocultures were analyzed for cytokine production by ELISA for IL-17A (BioLegend), TNF-α, IL-6, and IL-23 (R&D Systems) according to manufacturer's instructions.

Cell Lysates and Western Blotting. BmMs (10^7 cells/sample) were lysed by the addition of ice-cold, modified RIPA buffer (50 mM Tris, pH 7.4, 150 mM sodium chloride, 2% (v/v) NP-40, 0.25% (w/v) sodium deoxycholate, 1 mM EGTA, 10 mM sodium orthovanadate plus 0.5 mM phenylmethylsulfonyl fluoride, 10 μg/mL chymostatin, leupeptin, antipapain, and pepstatin) and solubilized on ice for 30 min. Protein (30 μg) samples were resolved on the XCell SureLock Mini-Cell kit with NuPAGE Novex high-performance precast Bis-Tris gels and NuPAGE buffers and reagents (Invitrogen Life Technologies) at 200 V for 50 min. Proteins were transferred to nitrocellulose (GE), and membranes were blocked by incubating for 1 h in 5% nonfat milk in TBS/Tween (0.5 M NaCl and 20 mM Tris pH7.5 with 0.1% (v/v) Tween-20) at RT. Membranes were incubated with primary antibody diluted in 5% BSA in TBS/Tween buffer overnight at 4 °C, washed with TBS/Tween, and incubated with the appropriate horseradish peroxidase (HRP)-conjugated secondary antibody in 5% nonfat milk for 1 h at RT. Membranes were then washed with TBS/Tween, and protein bands were visualized using the ECL detection system. Quantification of the bands was performed using ImageJ software (National Institutes of Health, USA).

Statistical Analysis of Data. Parametric data were analyzed by one-tailed Student's t test or by one-way ANOVA followed by Bonferroni's post-test. Normalized data were analyzed by the Kruskal−Wallis test, while the Mann−Whitney test was used for analysis of clinical CIA scores where *$p < 0.05$, **$p < 0.01$ and ***$p < 0.001$.

■ ASSOCIATED CONTENT

Ⓢ Supporting Information

Synthesis of compounds. This material is available free of charge via the Internet at http://pubs.acs.org.

■ AUTHOR INFORMATION

Corresponding Author

*Phone: 0044-141-548-3725. Fax: 0044-141-552-2562. E-mail: W.Harnett@strath.ac.uk.

Author Contributions

$\parallel$L.A.-R., M.A.P., and J.R. contributed equally to the work.

Notes

The authors declare no competing financial interest.

■ ACKNOWLEDGMENTS

■ ABBREVIATIONS USED

7-AAD, 7-Aminoactinomycin D; BLP, bacterial lipoprotein; bmDC, bone marrow-derived dendritic cell; bmM, bone marrow-derived macrophage; CIA, collagen-induced arthritis; *m*-CPBA, *meta*-chloroperbenzoic acid; CpG, cytosine-phosphate-guanine; DAMP, damage-associated molecular pattern; DLN, draining lymph node; HPLC, High performance liquid

chromatography; HRCIMS, high resolution chemical ionization mass spectroscopy; HREIMS, high resolution electron ionization mass spectroscopy; HRESIMS, high-resolution electrospray ionization mass spectroscopy; HRFABMS, high resolution fast atom bombardment mass spectroscopy; LPS, lipopolysaccharide; MyD88, myeloid differentiation primary response gene 88; OVA, ovalbumin; PAMP, pathogen-associated molecular pattern; PC, phosphorylcholine; PMA, phorbol myristate acetate; RA, rheumatoid arthritis; SMA, small molecule analogue

■ REFERENCES

(1) de Silva, N. R.; Brooker, S.; Hotez, P. J.; Montresor, A.; Engels, D.; Savioli, L. Soil-Transmitted Helminth Infections: Updating the Global Picture. *Trends Parasitol.* **2003**, *19*, 547−551.

(2) Hewitson, J. P.; Grainger, J. R.; Maizels, R. M. Helminth Immunoregulation: The Role of Parasite Secreted Proteins in Modulating Host Immunity. *Mol. Biochem. Parasitol.* **2009**, *167*, 1−11.

(3) Harnett, W.; Grainger, M.; Kapil, A.; Worms, M. J.; Parkhouse, R. M. E. Origin, Kinetics of Circulation and Fate in Vivo of the Major Excretory−Secretory Product of *Acanthocheilonema Viteae*. *Parasitol. Today* **1989**, *99*, 229−239.

(4) Goodridge, H. S.; Marshall, F. A.; Else, K. J.; Houston, K. M.; Egan, C.; Al-Riyami, L.; Liew, F. Y.; Harnett, W.; Harnett, M. M. Immunomodulation via Novel Use of TLR4 by the Filarial Nematode Phosphorylcholine-Containing Secreted Product, ES-62. *J. Immunol.* **2005**, *174*, 284−293.

(5) Goodridge, H. S.; McGuiness, S.; Houston, K. M.; Egan, C. A.; Al-Riyami, L.; Alcocer, M. J.; Harnett, M. M.; Harnett, W. Phosphorylcholine Mimics the Effects of ES-62 on Macrophages and Dendritic Cells. *Parasite Immunol.* **2007**, *29*, 127−137.

(6) Melendez, A. J.; Harnett, M. M.; Pushparaj, P. N.; Wong, W. S.; Tay, H. K.; McSharry, C. P.; Harnett, W. Inhibition of FcepsilonRI-Mediated Mast Cell Responses by ES-62, a Product of Parasitic Filarial Nematodes. *Nature Med.* **2007**, *13*, 1375−1381.

(7) McInnes, I. B.; Leung, B. P.; Harnett, M.; Gracie, J. A.; Liew, F. Y.; Harnett, W. A Novel Therapeutic Approach Targeting Articular Inflammation Using the Filarial Nematode-Derived Phosphorylcholine-Containing Glycoprotein ES-62. *J. Immunol.* **2003**, *171*, 2127−2133.

(8) Harnett, M. M.; Kean, D. E.; Boitelle, A.; McGuiness, S.; Thalhamer, T.; Steiger, C. N.; Egan, C.; Al-Riyami, L.; Alcocer, M. J.; Houston, K. M.; Gracie, J. A.; McInnes, I. B.; Harnett, W. The Phosphorycholine Moiety of the Filarial Nematode Immunomodulator ES-62 Is Responsible for Its Anti-Inflammatory Action in Arthritis. *Ann. Rheum. Dis.* **2008**, *67*, 518−523.

(9) Pineda, M. A.; McGrath, M. A.; Smith, P. C.; Al-Riyami, L.; Rzepecka, J.; Gracie, J. A.; Harnett, W.; Harnett, M. M. The Parasitic Helminth Product ES-62 Suppresses Pathogenesis in CIA by Targeting of the IL-17-Producing Cellular Network at Multiple Sites. *Arthritis Rheum.* **2012**, *64*, 3168−3178.

(10) Harnett, W.; Harnett, M. M.; Leung, B. P.; Gracie, J. A.; McInnes, I. B. The Anti-Inflammatory Potential of the Filarial Nematode Secreted Product, ES-62. *Curr. Top. Med. Chem.* **2004**, *4*, 553−559.

(11) Harnett, W.; Harnett, M. M. Immunomodulatory Activity and Therapeutic Potential of the Filarial Nematode Secreted Product, ES-62. *Adv. Exp. Med. Biol.* **2009**, *666*, 88−94.

(12) Kean, D. E.; Ohtsuka, I.; Sato, K.; Hada, N.; Takeda, T.; Lochnit, G.; Geyer, R.; Harnett, M. M.; Harnett, W. Dissecting Ascaris Glycosphingolipids for Immunomodulatory Moieties—The Use of Synthetic Structural Glycosphingolipid Analogues. *Parasite Immunol.* **2006**, *28*, 69−76.

(13) Harnett, W.; Harnett, M. M. Inhibition of Murine B Cell Proliferation and Down-Regulation of Protein Kinase C Levels by a Phosphorylcholine-Containing Filarial Excretory−Secretory Product. *J. Immunol.* **1993**, *151*, 4829−4837.

(14) Goodridge, H. S.; Marshall, F. A.; Wilson, E. H.; Houston, K. M.; Liew, F. Y.; Harnett, M. M.; Harnett, W. In Vivo Exposure of Murine Dendritic Cell and Macrophage Bone Marrow Progenitors to the Phosphorylcholine-Containing Filarial Nematode Glycoprotein ES-62 Polarizes Their Differentiation to an Anti-Inflammatory Phenotype. *Immunology* **2004**, *113*, 491−498.

(15) Deehan, M. R.; Goodridge, H. S.; Blair, D.; Lochnit, G.; Dennis, R. D.; Geyer, R.; Harnett, M. M.; Harnett, W. Immunomodulatory Properties of *Ascaris Suum* Glycosphingolipids—Phosphorylcholine and Non-Phosphorylcholine-Dependent Effects. *Parasite Immunol.* **2002**, *24*, 463−469.

(16) Lee, J. H.; Cho, M. L.; Kim, J. I.; Moon, Y. M.; Oh, H. J.; Kim, G. T.; Ryu, S.; Baek, S. H.; Lee, S. H.; Kim, H. Y.; Kim, S. I. Interleukin 17 (IL-17) Increases the Expression of Toll-Like Receptor-2, 4, and 9 by Increasing Il-1beta and Il-6 Production in Autoimmune Arthritis. *J. Rheumatol.* **2009**, *36*, 684−692.

(17) Ultaigh, S. N.; Saber, T. P.; McCormick, J.; Connolly, M.; Dellacasagrande, J.; Keogh, B.; McCormack, W.; Reilly, M.; O'Neill, L. A.; McGuirk, P.; Fearon, U.; Veale, D. J. Blockade of Toll-Like Receptor 2 Prevents Spontaneous Cytokine Release from Rheumatoid Arthritis ex Vivo Synovial Explant Cultures. *Arthritis Res. Ther.* **2011**, *13*, R33.

(18) Saber, T.; Veale, D. J.; Balogh, E.; McCormick, J.; NicAnUltaigh, S.; Connolly, M.; Fearon, U. Toll-Like Receptor 2 Induced Angiogenesis and Invasion Is Mediated through the Tie2 Signalling Pathway in Rheumatoid Arthritis. *PLoS One* **2011**, *6*, e23540.

(19) Bobacz, K.; Sunk, I. G.; Hofstaetter, J. G.; Amoyo, L.; Toma, C. D.; Akira, S.; Weichhart, T.; Saemann, M.; Smolen, J. S. Toll-Like Receptors and Chondrocytes: The Lipopolysaccharide-Induced Decrease in Cartilage Matrix Synthesis Is Dependent on the Presence of Toll-Like Receptor 4 and Antagonized by Bone Morphogenetic Protein 7. *Arthritis Rheum.* **2007**, *56*, 1880−1893.

(20) Goh, F. G.; Midwood, K. S. Intrinsic Danger: Activation of Toll-Like Receptors in Rheumatoid Arthritis. *Rheumatology (Oxford, U. K.)* **2012**, *51*, 7−23.

(21) Huang, Q. Q.; Pope, R. M. The Role of Toll-Like Receptors in Rheumatoid Arthritis. *Curr. Rheumatol. Rep.* **2009**, *11*, 357−364.

(22) Abdollahi-Roodsaz, S.; van de Loo, F. A.; van den Berg, W. B. Trapped in a Vicious Loop: Toll-Like Receptors Sustain the Spontaneous Cytokine Production by Rheumatoid Synovium. *Arthritis Res. Ther.* **2011**, *13*, 105.

(23) Hennessy, E. J.; Parker, A. E.; O'Neill, L. A. Targeting Toll-Like Receptors: Emerging Therapeutics? *Nature Rev. Drug Discovery* **2010**, *9*, 293−307.

(24) Whelan, M.; Harnett, M. M.; Houston, K. M.; Patel, V.; Harnett, W.; Rigley, K. P. A Filarial Nematode-Secreted Product Signals Dendritic Cells to Acquire a Phenotype That Drives Development of Th2 Cells. *J. Immunol.* **2000**, *164*, 6453−6460.

(25) Kapadnis, P. B.; Hall, E.; Ramstedt, M.; Galloway, W. R.; Welch, M.; Spring, D. R. Towards Quorum-Quenching Catalytic Antibodies. *Chem. Commun. (Cambridge, U. K.)* **2009**, 538−540.

(26) Ettari, R.; Bonaccorso, C.; Micale, N.; Heindl, C.; Schirmeister, T.; Calabro, M. L.; Grasso, S.; Zappala, M. Development of Novel Peptidomimetics Containing a Vinyl Sulfone Moiety as Proteasome Inhibitors. *ChemMedChem* **2011**, *6*, 1228−1237.

(27) Santos, M. M.; Moreira, R. Michael Acceptors as Cysteine Protease Inhibitors. *Mini-Rev. Med. Chem.* **2007**, *7*, 1040−1050.

(28) Guay, D.; Beaulieu, C.; Percival, M. D. Therapeutic Utility and Medicinal Chemistry of Cathepsin C Inhibitors. *Curr. Top. Med. Chem.* **2010**, *10*, 708−716.

(29) Fairlamb, I. J.; Dickinson, J. M.; O'Connor, R.; Cohen, L. H.; van Thiel, C. F. Synthesis and Antimicrobial Evaluation of Farnesyl Diphosphate Mimetics. *Bioorg. Chem.* **2003**, *31*, 80−97.

(30) Perruchon, J.; Ortmann, R.; Altenkamper, M.; Silber, K.; Wiesner, J.; Jomaa, H.; Klebe, G.; Schlitzer, M. Studies Addressing the Importance of Charge in the Binding of Fosmidomycin-Like Molecules to Deoxyxylulosephosphate Reductoisomerase. *ChemMedChem* **2008**, *3*, 1232−1241.

(31) Sennhenn, P.; Mantoulidis, A.; Treu, M.; Tontsch-Grunt, U.; Spevak, W.; McConnell, D.; Schoop, A.; Bruckner, R.; Jacobi, A.; Gurler, U.; Schnapp, G.; Klein, C.; Himmelsbach, F.; Pautsch, A.; Betzemeier, B.; Herfurth, L.; Mack, J.; Wiedenmayer, D.; Bader, G.; Reiser, U. Alpha-Carbolines as Cdk-1 Inhibitors. WO/2006/131552, 2006.

(32) Bursavich, M. G.; Chen, L.; Gilbert, A. M.; Hu, Y.; Jennings, L. D.; Kincaid, S. L.; Powell, D. W.; Sum, F.-W.; Zhang, Y. Anilino-Pyrimidine Analogs. US 2010 7799915, 2010.

(33) Lim, C.; Lee, M.; Park, E. J.; Cho, R.; Park, H. J.; Lee, S. J.; Cho, H.; Lee, S. K.; Kim, S. Sulfonamide Derivatives of Styrylheterocycles as a Potent Inhibitor of Cox-2-Mediated Prostaglandin E2 Production. *Bioorg. Med. Chem. Lett.* **2010**, *20*, 6938−6941.

(34) Lee, K. L.; Foley, M. A.; Chen, L.; Behnke, M. L.; Lovering, F. E.; Kirincich, S. J.; Wang, W.; Shim, J.; Tam, S.; Shen, M. W.; Khor, S.; Xu, X.; Goodwin, D. G.; Ramarao, M. K.; Nickerson-Nutter, C.; Donahue, F.; Ku, M. S.; Clark, J. D.; McKew, J. C. Discovery of Ecopladib, an Indole Inhibitor of Cytosolic Phospholipase A2alpha. *J. Med. Chem.* **2007**, *50*, 1380−1400.

(35) McKew, J. C.; Lee, K. L.; Shen, M. W.; Thakker, P.; Foley, M. A.; Behnke, M. L.; Hu, B.; Sum, F. W.; Tam, S.; Hu, Y.; Chen, L.; Kirincich, S. J.; Michalak, R.; Thomason, J.; Ipek, M.; Wu, K.; Wooder, L.; Ramarao, M. K.; Murphy, E. A.; Goodwin, D. G.; Albert, L.; Xu, X.; Donahue, F.; Ku, M. S.; Keith, J.; Nickerson-Nutter, C. L.; Abraham, W. M.; Williams, C.; Hegen, M.; Clark, J. D. Indole Cytosolic Phospholipase A2 Alpha Inhibitors: Discovery and in Vitro and in Vivo Characterization of 4-{3-[5-Chloro-2-(2-{[(3,4-dichlorobenzyl)-sulfonyl]amino}ethyl)-1-(diphenylmethyl)-1*H*-indol-3-yl]propyl}-benzoic Acid, Efipladib. *J. Med. Chem.* **2008**, *51*, 3388−3413.

(36) Smits, R. A.; Adami, M.; Istyastono, E. P.; Zuiderveld, O. P.; van Dam, C. M.; de Kanter, F. J.; Jongejan, A.; Coruzzi, G.; Leurs, R.; de Esch, I. J. Synthesis and Qsar of Quinazoline Sulfonamides as Highly Potent Human Histamine H4 Receptor Inverse Agonists. *J. Med. Chem.* **2010**, *53*, 2390−2400.

(37) Goodridge, H. S.; Harnett, W.; Liew, F. Y.; Harnett, M. M. Differential Regulation of Interleukin-12 p40 and p35 Induction Via Erk Mitogen-Activated Protein Kinase-Dependent and -Independent Mechanisms and the Implications for Bioactive IL-12 and IL-23 Responses. *Immunology* **2003**, *109*, 415−425.

(38) Goodridge, H. S.; Wilson, E. H.; Harnett, W.; Campbell, C. C.; Harnett, M. M.; Liew, F. Y. Modulation of Macrophage Cytokine Production by ES-62, a Secreted Product of the Filarial Nematode *Acanthocheilonema Viteae. J. Immunol.* **2001**, *167*, 940−945.

(39) Harnett, W.; Harnett, M. M.; Byron, O. Structural/Functional Aspects of ES-62-a Secreted Immunomodulatory Phosphorylcholine-Containing Filarial Nematode Glycoprotein. *Curr. Protein Pept. Sci.* **2003**, *4*, 59−71.

(40) Goodridge, H. S.; Stepek, G.; Harnett, W.; Harnett, M. M. Signalling Mechanisms Underlying Subversion of the Immune Response by the Filarial Nematode Secreted Product ES-62. *Immunology* **2005**, *115*, 296−304.

(41) Li, R.; Zheng, X.; Popov, I.; Zhang, X.; Wang, H.; Suzuki, M.; Necochea-Campion, R. D.; French, P. W.; Chen, D.; Siu, L.; Koos, D.; Inman, R. D.; Min, W. P. Gene Silencing of IL-12 in Dendritic Cells Inhibits Autoimmune Arthritis. *J. Transl. Med.* **2012**, *10*, 19.

(42) Benson, J. M.; Peritt, D.; Scallon, B. J.; Heavner, G. A.; Shealy, D. J.; Giles-Komar, J. M.; Mascelli, M. A. Discovery and Mechanism of Ustekinumab: A Human Monoclonal Antibody Targeting Interleukin-12 and Interleukin-23 for Treatment of Immune-Mediated Disorders. *mAbs* **2011**, *3*, 535−545.

(43) Tang, C.; Chen, S.; Qian, H.; Huang, W. Interleukin-23: As a Drug Target for Autoimmune Inflammatory Diseases. *Immunology* **2012**, *135*, 112−124.

(44) Alonzi, T.; Fattori, E.; Lazzaro, D.; Costa, P.; Probert, L.; Kollias, G.; De Benedetti, F.; Poli, V.; Ciliberto, G. Interleukin 6 Is Required for the Development of Collagen-Induced Arthritis. *J. Exp. Med.* **1998**, *187*, 461−468.

(45) Scott, D. L. Biologics-Based Therapy for the Treatment of Rheumatoid Arthritis. *Clin. Pharmacol. Ther.* **2012**, *91*, 30−43.

(46) Kanayama, M.; Morimoto, J.; Matsui, Y.; Ikesue, M.; Danzaki, K.; Kurotaki, D.; Ito, K.; Yoshida, T.; Uede, T. Alpha9beta1 Integrin-Mediated Signaling Serves as an Intrinsic Regulator of Pathogenic Th17 Cell Generation. *J. Immunol.* **2011**, *187*, 5851−5864.

(47) Mu, H. H.; Hasebe, A.; Van Schelt, A.; Cole, B. C. Novel Interactions of a Microbial Superantigen with TLR2 and TLR4 Differentially Regulate IL-17 and Th17-Associated Cytokines. *Cell. Microbiol.* **2011**, *13*, 374−387.

(48) He, Z.; Shotorbani, S. S.; Jiao, Z.; Su, Z.; Tong, J.; Liu, Y.; Shen, P.; Ma, J.; Gao, J.; Wang, T.; Xia, S.; Shao, Q.; Wang, S.; Xu, H. HMGB1 Promotes the Differentiation of Th17 Via up-Regulating TLR2 and IL-23 of CD14(+) Monocytes from Patients with Rheumatoid Arthritis. *Scand. J. Immunol.* **2012**, *76*, 483−490.

(49) Goodridge, H. S.; Deehan, M. R.; Harnett, W.; Harnett, M. M. Subversion of Immunological Signalling by a Filarial Nematode Phosphorylcholine-Containing Secreted Product. *Cell. Signalling* **2005**, *17*, 11−16.

(50) Papp, K. A.; Langley, R. G.; Sigurgeirsson, B.; Abe, M.; Baker, D. R.; Konno, P.; Haemmerle, S.; Thurston, H. J.; Papavassilis, C.; Richards, H. B. Efficacy and Safety of Secukinumab in the Treatment of Moderate-to-Severe Plaque Psoriasis: A Randomized, Double-Blind, Placebo-Controlled Phase II Dose-Ranging Study. *Br. J. Dermatol.* **2013**, *168*, 412−421.

(51) Papp, K. A.; Leonardi, C.; Menter, A.; Ortonne, J. P.; Krueger, J. G.; Kricorian, G.; Aras, G.; Li, J.; Russell, C. B.; Thompson, E. H.; Baumgartner, S. Brodalumab, an Anti-Interleukin-17-Receptor Antibody for Psoriasis. *N. Engl. J. Med.* **2012**, *366*, 1181−1189.

(52) Spuls, P. I.; Hooft, L. Brodalumab and Ixekizumab, Anti-Interleukin-17-Receptor Antibodies for Psoriasis: A Critical Appraisal. *Br. J. Dermatol.* **2012**, *167*, 710−713 discussion pp 714−715..

(53) Ball, D. H.; Tay, H. K.; Bell, K. S.; Coates, M. L.; Al-Riyami, L.; Rzepecka, J.; Harnett, W.; Harnett, M. M. Mast Cell Subsets and Their Functional Modulation by the *Acanthocheilonmea Viteae* Product, ES-62. *J.Parasitol. Res.* **2013**, *2013*, 13.

(54) Abdollahi-Roodsaz, S.; van de Loo, F. A.; Koenders, M. I.; Helsen, M. M.; Walgreen, B.; van den Bersselaar, L. A.; Arntz, O. J.; Takahashi, N.; Joosten, L. A.; van den Berg, W. B. Destructive Role of Myeloid Differentiation Factor 88 and Protective Role of Trif in Interleukin-17-Dependent Arthritis in Mice. *Arthritis Rheum.* **2012**, *64*, 1838−1847.

(55) Zhu, W.; London, N. R.; Gibson, C. C.; Davis, C. T.; Tong, Z.; Sorensen, L. K.; Shi, D. S.; Guo, J.; Smith, M. C.; Grossmann, A. H.; Thomas, K. R.; Li, D. Y. Interleukin Receptor Activates a Myd88-Arno-Arf6 Cascade to Disrupt Vascular Stability. *Nature* **2012**, *492*, 252−255.

(56) Thomas, P. G.; Carter, M. R.; Atochina, O.; Da'Dara, A. A.; Piskorska, D.; McGuire, E.; Harn, D. A. Maturation of Dendritic Cell 2 Phenotype by a Helminth Glycan Uses a Toll-Like Receptor 4-Dependent Mechanism. *J. Immunol.* **2003**, *171*, 5837−5841.

(57) van der Kleij, D.; Latz, E.; Brouwers, J. F.; Kruize, Y. C.; Schmitz, M.; Kurt-Jones, E. A.; Espevik, T.; de Jong, E. C.; Kapsenberg, M. L.; Golenbock, D. T.; Tielens, A. G.; Yazdanbakhsh, M. A Novel Host−Parasite Lipid Cross-Talk. Schistosomal Lyso-Phosphatidylserine Activates Toll-Like Receptor 2 and Affects Immune Polarization. *J. Biol. Chem.* **2002**, *277*, 48122−48129.

(58) Al-Riyami, L.; Harnett, W. Immunomodulatory Properties of ES-62, a Phosphorylcholine-Containing Glycoprotein Secreted by *Acanthocheilonema Viteae. Endocr. Metab. Immune Disord. Drug Targets* **2012**, *12*, 45−52.

(59) Erb, K. J. Can Helminths or Helminth-Derived Products Be Used in Humans to Prevent or Treat Allergic Diseases? *Trends Immunol.* **2009**, *30*, 75−82.

(60) Houston, K. M.; Babayan, S. A.; Allen, J. E.; Harnett, W. Does *Litomosoides sigmodontis* Synthesize Dimethylethanolamine from Choline? *Parasitology* **2008**, *135*, 55−61.

(61) Frostegard, J. Low Level Natural Antibodies against Phosphorylcholine: A Novel Risk Marker and Potential Mechanism in Atherosclerosis and Cardiovascular Disease. *Clin. Immunol.* **2010**, *134*, 47−54.

(62) Sorensen, T. J.; Nielsen, M. F. Synthesis, Uv/Vis Spectra and Electrochemical Chaarcaterisation of Arylthio and Styryl Substituted Ferrocenes. *Cent. Eur. J. Chem.* **2011**, *9*, 610−618.

(63) Choong, C.; Foord, J. S.; Griffiths, J. P.; Parker, E. M.; Baiwen, L.; Bora, M.; Moloney, M. G. Post-Polymerisation Modification of Surface Chemical Functionality and Its Effect on Protein Binding. *New J. Chem.* **2012**, *36*, 1187−1200.

(64) Sontag, S. K.; Sheppard, G. R.; Usselman, N. M.; Marshall, N.; Locklin, J. Surface-Confined Nickel Mediated Cross-Coupling Reactions: Characterization of Initiator Environment in Kumada Catalyst-Transfer Polycondensation. *Langmuir* **2011**, *27*, 12033−12041.

(65) Rafikov, S. R.; Ergebekov, M. E. Synthesis of *p*-Methylbenzyl-phosphonic Acid. *Zh. Obshch. Khim.* **1964**, *34*, 2230−2233.

(66) Okamato, Y.; Iwamoto, N.; Takamuku, S. Photochemical Carbon−Phosphorus Bond Cleavage of Nitro-Substituted Benzyl-phosphonic Acids. *J. Chem. Soc., Chem. Commun.* **1986**, 1516−1517.

(67) Dolaz, M.; Yilmaz, H. Characterisation and Applications of New Azo Compounds Containing Phosphonic Acid. *Asian J. Chem.* **2009**, *21*, 59085−55094.

(68) Meutermans, W. D. F.; Golding, S. W.; Bourne, G. T.; Miranda, L. P.; Dooley, M. J.; Alewood, P. F.; Smythe, M. L. Synthesis of Difficult Cyclic Peptides by Inclusion of a Novel Photolabile Auxiliary in a Ring Contraction Strategy. *J. Am. Chem. Soc.* **1999**, *121*, 9790−9796.

(69) Kotsova, A. G.; Shvetsova, L. S.; Kalganova, I. I. Alkanesulfonic Acids. XII. The Reaction of 2-Chloroethanesulfonyl Chloride with Aromatic Amines. *Zh. Obshch. Khim.* **1954**, *24*, 1397−1402.

(70) Preparation of Organic Ammonium Compounds. (Farbwerke Hoechst AG) . BE632987 1963.

(71) Ono, S.; Yamafuji, T.; Chaki, H.; Todo, Y.; Maekawa, M.; Kitamura, K.; Tai, M.; Narita, H. Studies on Cognitive Enhancing Agents. I. Antiamnestic and Antihypoxic Activities of 2-Dimethylami-noethyl Ethers and Related Compounds. *Chem. Pharm. Bull. (Tokyo)* **1995**, *43*, 1483−1487.

(72) Legheand, J.; Cuisinaud, G.; Sabbagh, M.; Pabiot, N.; Seccia, M.; Cier, A. Pharmacological Study of Various *N*-Amide Derivatives of *N′,N′*-Disubstituted Ethylene Diamine. *Ann. Pharm. Fr.* **1977**, *35*, 45−51.